EDUCTION BEHAVIOUR IN IRON ORE-CHAR MIXTURE N ARGON AND HYDROGEN-CARBON DIOXIDE GASES

by

KAPIL DEO

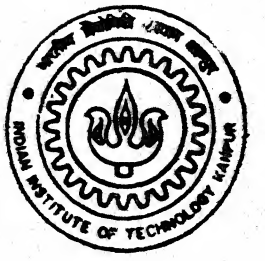

Department of Materials and Metallurgical Engineering

INDIAN INSTITUTE OF TECHNOLOGY KANPUR

December 1999

REDUCTION BEHAVIOUR IN IRON ORE-CHAR MIXTURE IN ARGON AND HYDROGEN-CARBON DIOXIDE GASES

A Thesis submitted

in Partial Fulfillment of the Requirements

for the Degree of

Master of Technology

by

KAPIL DEO

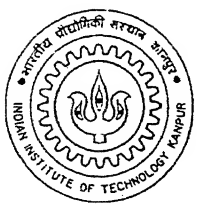

to the

DEPARTMENT OF MATERIALS AND METALLURGICAL ENGINEERING
INDIAN INSTITUTE OF TECHNOLOGY KANPUR

DECEMBER 1999

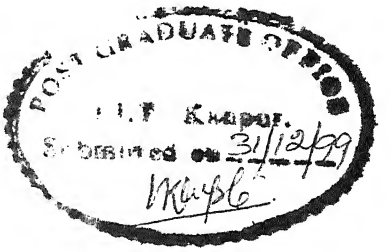

CERTIFICATE

It is certified that the work contained in this thesis entitled "*Reduction behaviour in iron ore-air mixture in argon and hydrogen-carbon dioxide gases*", by Kapil Deo, has been carried out under my supervision and that this work has not been submitted elsewhere for any degree.

Dr. A.GHOSH
Professor
Materials and Metallurgical Engineering,
Indian Institute of Technology, Kanpur
December, 1999

Dedicated to .....

My Grandparents

Acknowledgement

I thank my guide, Prof. A.Ghosh, for his guidance, inspiration and encouragement during t course of this project. He has taught me the values of research and independent thinking. He spe tremendous time and effort on me and was always ready to help and discuss my difficulties. It w a great pleasure working with him.

I must take the opportunity to thank my friends Ashish, Binod, Sanjay, Kalpesh, Badirujjam Rajiv, Shoumitra, Saurabh and Saumya for their kind help in completing this thesis. I also wo like to thank all the laboratory staffs, Mr.A.Sharma and Mr.Ramavtar who have helped me a l without which this thesis could not have been a reality. Finally I must thank my lab-mates A and Lawania for their kind support to successfully complete this work.

CONTENTS

LIST OF TABLES

LIST OF FIGURES

ABSTRACT

In the past there had been fundamental studies on kinetics of reduction of iron oxide by carbon in mixtures of fines of these. The experiments were conducted in either inert atmosphere or under vacuum at high temperature. In recent years, cold-bonded composite iron ore – reductant pellets, consisting of mixtures of fines, seem to have considerable future potential as providing one of the alternative iron making routes. These pellets are reduced in industrial furnaces under reactive atmosphere resulting from combustion of carbon/hydrocarbons.

The present investigation has relevance to this. It is a fundamental study on kinetics of reduction of iron oxide in a powder mixture of blue dust and activated char, both under argon as well as under reactive gas mixtures at 1150, 1250, and 1300 K. The reactive gases were generated by introducing mixtures of H_2 and CO_2 in the ratios of H_2/CO_2 equal to 3 and 1.5. Due to water gas shift reaction, it generates a gas mixture consisting of H_2, H_2O, CO and CO_2 at high temperature in reduction furnace. Influence of variables, viz. Fe_2O_3/C ratio and size of the sample was also investigated. The experiments were conducted for durations of 600, 1200, 1800, 2400, and 3000 seconds of the sample in the hot zone.

The data on degree of reduction (F) versus time were fitted by polynomial through regression analysis. F versus t data show for most cases highest degree of reduction for inlet gas of H_2/CO_2 ratio equal to 3, and lowest values of F for H_2/CO_2 ratio of 1.5. In argon, the values of F in most cases are somewhere in between the above two. This may be explained by the fact that, thermodynamically speaking, the gas mixture with H_2/CO_2 ratio of 3, is reducing to wustite. On the other hand, the mixture with H_2/CO_2 equal to 1.5 is oxidising to wustite. However, in some situations, there were departures from this, and attempts were made to explain the same as possible. An interesting finding is that, at 1300 K, the oxide got reduced almost completely even under a gas mixture of H_2/CO_2 ratio of 1.5.

Chapter 1

INTRODUCTION

1.1 : Introductory

With the passage of years, electric arc furnaces (EAF) are growing in popularity. The principal metallic feed is steel scrap. Recently there is a large scale shortage of scrap World wide as well as in India. The shortage is going to increase in future. This led to the growth of sponge iron making processes, because sponge iron is a substitute for steel scrap.

Blast furnace is the principal route of iron making. However due to large capital investment, shortage and cost of metallurgical coking coal as well as environmental pollution during coke making, there is a Worldwide thrust to develop smaller units of alternative method for the production of liquid iron in order to supplement blast furnace iron making.

A very promising route of alternative iron making is use of composite pellets of iron ore and reductant (coal, char, coke fines), which are imparted sufficient green strength for handling by cold bonding.

Advantages are :

(a) Use of cheap raw materials, viz., ore fines, mill scale, non coking coal fines etc.

(b) very fast reduction in mixtures of fines of ore and carbon.

The present study is concerned with reduction behaviour in mixture of iron ore and carbon in various gaseous environment. It is relevent to alternative iron making through composite pellet route.

Chapter 2 reviews alternative iron making processes. There have been several fundamental investigations on mixtures of fines of iron oxide/ore and carbon. These have been reviewed in detail elsewhere[1]. Therefore only an outline of the latter is being noted below.

1.2 : Outline of earlier studies on fundamentals of carbothermic reduction

Most of the fundamental studies have been conducted with intimately mixed fines of oxide and carbon.

The overall reduction reaction may be represented as :

$$mFe_xO_y(s) + C(s) = nFe_zO_w(s) + CO(g) \qquad (1.1)$$

The reason for using symbols x, y, z, w is that there are three oxides of iron, viz; Fe_2O_3, Fe_3O_4, Fe_xO. It is well established that reduction of iron oxides by carbon occurs as a combination of the following gas-solid reactions.

Gasification of carbon : $C(s) + CO_2(g) = 2CO(g)$ (1.2)

Reduction of iron oxides by CO, viz

$$3Fe_2O_3(s) + CO(g) = 2Fe_3O_4 + CO_2(g) \qquad (1.3)$$

$$Fe_3O_4(s) + CO(g) = 3FeO(s) + CO_2(g) \qquad (1.4)$$

$$FeO(s) + CO(g) = Fe(s) + CO_2(g) \qquad (1\ 5)$$

Actually, FeO is non-stoichiometric oxide and be better represented as Fe_xO, where x is a variable ranging from 0.87 to 0.955, depending on oxygen potential and temperature. However in order to avoid complications, it has been represented as FeO in Eqs. (1.4) and (1.5).

Kinetically a solid-solid reaction is expected to be much slower compared to a gas-solid reaction. This is because of the following reasons.

(a) Solid-solid contact area is much smaller than that of gas-solid one.

(b) solid state diffusion is much slower than that of gaseous diffusion.

Therefore, it is more likely that the reduction of iron oxide by carbon in mixture of fines will occur via the two component reaction, viz; reduction of iron oxides by carbon monoxide, and gasification of carbon by CO_2. Investigations have confirmed it through experiments.

The variables which have been found to influence the reduction rates of iron oxide by carbon are :

(a) Temperature

(b) nature of carbon

(c) particle size

(d) carbon/oxide ratio

(e) presence of catalyst/inhibitors

It has been established by several investigators that reduction of iron oxides by carbon is dominantly controlled by rate of gassification of carbon. The gasification reaction is primarily controlled by slow chemical reaction step.

Evidences are :

(a) high activation energy

(b) catalytic effect of metallic iron, alkalies etc.

(c) inhibiting effect of CO, some sulphides

(d) largely uniform internal reaction.

Similarly, temperature has a pronounced effect on the carbothermic reduction rate. Activation energy generally varies over a wide range starting from 56 KJ/mol to 418 KJ/mol. The early stage of reduction is characterised by high activation energy (240-300 KJ/mol) indicating that it is controlled by gasification reaction, since activation energy for reduction for reduction reaction varies approximately between 40-100 KJ/mol only.

For mixture of fines of oxide and carbon, the later stage is associated with much lower activation energy. A strong enhancement of rate is also exhibited. These have been explained by formation of metallic iron due to reduction, and its catalytic effect on gasification reaction. Lastly, some quantitative correlations between rates of gasification reaction and then of reduction of iron oxide by carbon have also been reported in the literature.

1.3 : Work Plan

In alternative iron making through composite pellet route, the pellets are reduced in reactive atmosphere consisting of CO, CO_2, H_2 and H_2O etc. Most of the fundamental studies on mixtures of fines of iron oxide/ore and carbon with or without binder were carried out under inert atmosphere. Hence it was

decided that besides argon other gaseous environments will be employed. Due to ease of availability and handling, carbondioxide and hydrogen were chosen as other gases. A mixture of CO_2 and H_2 undergoes the water gas shift reaction viz.

$$CO_2(g) + H_2(g) = CO(g) + H_2O(g) \qquad (1.6)$$

It has been established that this reaction attains equilibrium very fast at high temperature resulting into a known mixture of CO, CO_2, H_2, and H_2O.

India has a large reserve of iron ore fines of high grade iron ore known as "blue dust". There have been studies on composite pellets using blue dust earlier in this laboratory and elsewhere. Hence some backup data are available also. So it was used for studies here.

Reactivity of carbon is an important parameter. It was decided to employ activated char which has high reactivity. In other study investigations have been done with graphite, which has a low reactivity, for comparision.

For proper interpretation controlled cylindrical geometry was employed. The trials were given with inorganic binders, since organic binders would complicate interpretations. However it was not possible to achieve sufficient green strength for handling.

Influence of following variables were investigated.

(a) Gas composition

(b) temperature

(c) size of the sample

(d) Fe_2O_3/C ratio

(e) time of reduction.

The method was to weigh samples before and after reduction. This was supplemented by separate determination of degree of reduction.

Chapter 2

LITERATURE REVIEW ON ALTERNATIVE IRON MAKING

As stated in chapter 1, the present investigation is fundamental in nature. Technologically it has special relevance to alternative iron making via the composite pellet route. Over a period of several decades a large number of alternative iron making processes have been developed. Only a few of them have been commercially successful. New processes are all the time being developed. This requires that we keep ourselves updated with the status of alternative iron making processes. Hence it was decided to include this chapter in the thesis.

2.1 : Introduction[2]

Blast furnace is the most important reactor for iron making, and is going to remain the dominant process in forseeable future as well. However due to :

(a) World wide shortage of metallurgical coking coal

(b) cost and environmental pollution of coke making

(c) need for smaller units requiring less capital and allowing dispersion of iron making facility,

Search for iron making processes, alternative to blast furnace, has been there for many decades.

In the Indian context, there are various reasons which lead to an increase in demand of alternative iron making processes. The reasons can be explained as follows :

(a) Country has abundant reserve of iron ore and non coking coal. Since the alternative iron making processes utilise coal of various grades, they can be used extensively in large scale for iron making.

(b) Due to modern technologies involved in iron and steel making, steel plant yield has increased, thus decreasing the extent of scrap generation. Since scrap is one of the important charge materials in steel making, its shortage imposes certain restrictions in producing steel by conventional steel making processes. So there is an increase in demand of DRI/HBI as an alternate charge material.

As already stated, in the last 60 years or so, innumerable alternative iron making processes producing either sponge iron or liquid iron have been patented. However very few of them have eventually got established as commercially viable. A look at technical journals reveals that even now processes are being developed. It is an ongoing exercise. As science and engineering make advances, situations with respect to raw materials, economic and social factors keep changing. More superior processes keep coming up making some of the older ones less viable.

2.2 : Alternative Iron making processes for Sponge iron making

2.2.1: General

Sponge iron is the iron produced in solid state at a temperature lower than 1100^0C. When a piece of iron ore is reduced the resulting sponge iron is porous. It is commercially known as "Directly Reduced Iron (DRI)". The porous nature poses two problems.

(a) The bulk density is low, requiring more volume for storage, transportation etc.

(b) Due to high specific surface area DRI gets easily reoxidised. As a matter of fact, it sometimes behaves as a pyrophoric material if not handled properly.

In order to avoid the above difficulties many sponge iron manufacturers briquette DRI at high pressure and in hot condition to produce a compact, denser solid. This is known as "Hot Briquetted Iron (HBI)".

Sponge iron making is very old and was the form in which iron used to be produced in early days. Production of liquid iron started with the advent of shaft/Blast Furnace in the 14^{th} century in Europe. Table 2.1 presents a brief summary of iron making technologies over centuries.

Data on demand and supply of scrap, DRI/HBI as well as projections for the future for the World and India are available. This shows that for the year 2000-2010 AD there will be considerable shortage of scrap both in India as well as in the World. This shortage is predicted to be so much that the current rate of growth of DRI/HBI production would not be able to cope up with the supply of

Table 2.1 : Iron Making Technologies over Centuries

PERIOD	TECHNOLOGY	State of Iron Produced	FUEL USED	Is fuel eco-friendly And renewable?
2000 BC - 1300 AD	Small scale & Tribal	Solid & Semi-solid	Wood Char	Yes
1300 AD - 1700 AD	Shaft / Blast Furnace	Semi solid / Liquid	Wood Char	Yes
1700 AD - 1900 AD	Blast Furnace	Liquid	Wood char / Coke	Partial
1900 AD - 1950 AD	Blast furnace	Liquid	Coke	No
1950 AD - 2000 AD	Blast furnace	Liquid	Coke	No
	DRI	Sponge	Coal / Gas	No
	Smelting Reduction	Liquid	Coal / Oxy	No
2000 AD - 2010 AD (speculated)	Blast Furnace	Liquid	Coke	No
	DRI	Sponge	Coal / Gas	No
	Smelting Reduction	Liquid	Coal / Oxy	No
	Blast Furnace	Liquid	Wood Char ?	Yes

metallics for steel making. Table 2.2 presents data. There has been considerable growth of DRI/HBI production in India in the present decade as shown in Table 2.3. Even with this impressive growth the anticipated shortfall in DRI/HBI will be estimated as 1.5 Mt in 2000-02 and 8Mt in 2006-07. Hence it is necessary for India to have good growth in the area of DRI/HBI production.

Basic features of reactors used for alternative iron making are presented in Table 2.4. It includes both sponge iron making as well as liquid iron making. The four basic reactor types for sponge iron making are schematically shown in Fig 2.1. The basic features of currently patented processes are presented in Table 2.5.

Table 2.5 lists a number of sponge iron processes including production of iron powder. Out of these only a few are currently commercially established. Most important tonnage wise is the Midrex process, followed by HYL, Rotary Kiln, Finmet and Nu-Iron process. Fig 2.2 shows the situation schematically, indicating the types of feed they use and current commercial status.

2.2.2 : Midrex Process

Since the start-up of the first[3] MIDREX Direct Reduction Plant in 1969, plant capacities have steadily increased in order to provide improved economy of scale, and to satisfy increasing Worldwide demand for DRI.

The process essentially consists of reducing the ore pellets by reformed natural gas in a vertical shaft furnace. Reforming reactions are carried out in a separate furnace, and are as follows:

Table 2.2 : Anticipated World short-fall in scrap and DRI/HBI [28]

	2000 (MT)	2005 (MT)	2010 (MT)
Demand of steel scrap and DRI/HBI	440	510	618
Likely availability of scrap	327	332	336
Likely availability of DRI/HBI	50	53	53
Short-fall of metallics in EAF	(-)63	(-)125	(-)229

Table 2.3 : DRI/HBI growth rate – World and India [28]

YEAR	World Production (MT)	Growth (%)	Production in India (MT)	Growth (%)
1992	20.42		1.44	
1993	23.74		2.21	
1994	27.53	11.9	2.91	29.5
1995	31.15		4.27	
1996	32.83		4.79	
1997	35.70		5.25	

Table 2.4 : Basic Features of Reactors Used for Iron Making [23]

Parameters	Shaft	Retort	Fluid Bed	Rotary Kiln	Rotary Hearth	Electric F/C	Smelting Unit
Ore	Pellet	Pellet	Fine	Lump, Pellet	Fine, Pellet	Fine, Pellet	Lump, Pellet
Reductant	Natural Gas	Natural Gas, Coal	Natural Gas	Coal	Coal	Coke, Char Wood char	Coal
Energy	Natural Gas	Natural Gas	Natural Gas	Natural Gas Pulverised Coal	Producer Gas, Oil, By-Prod. Gas	Electrical, Oxygen	Coal, Oxygen
Product	Sponge, HBI	Sponge, HBI	Iron Powder	Sponge	Sponge, Iron Fines	Liquid Iron	Liquid Iron
Process	Continuous	Batch	Continuous	Continuous	Continuous	Continuou, Batch	Continuous
Heat Transfer	Best	Very Good-Poor	Best	Good	Good	Best	Best
Volume Use	Maximum	Maximum	Very Less	Less	Less	High	Very Less
Limitation	Gas Based	Sponge Fusion	Low Productivity	Ring Formation	Small scale Operation	Power Based	Quality of Raw Material
Best Merit	Easy maintenance	Good product Quality control	Use of fine Ore	Use of coal as fuel	Use of coal & ore fines	Liquid Product	Liquid iron using coal

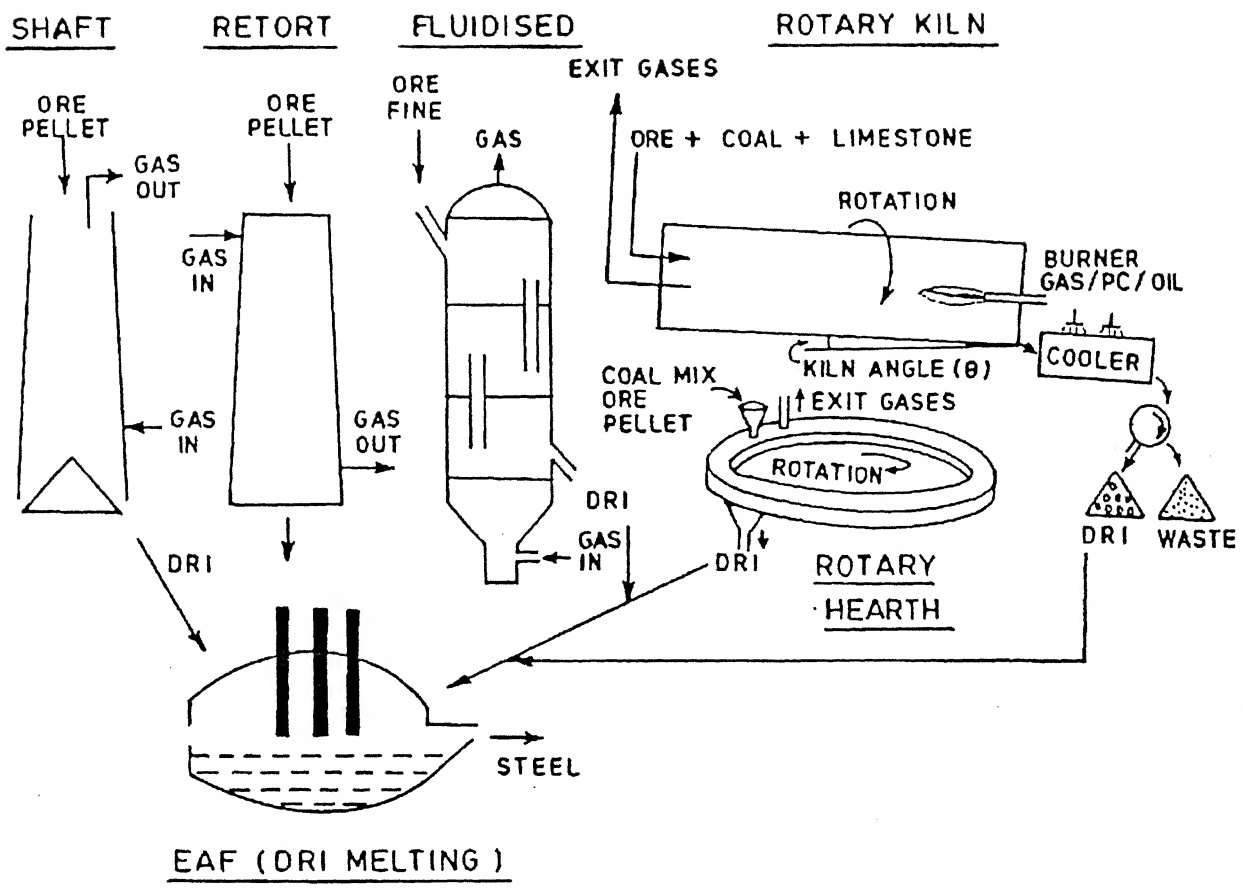

Fig. 2.1 : Reactors for alternate iron making technology. [23]

Table 2.5 : Basic Features of Some Alternate Iron Making Units [23]

PPROCESS	Basic Features of Alternate Iron Making Methods				Year	Country
	Reductant	Ore Form	Reactor	Product		
Hoganas	coke br.	fine	Retort	powder	1910	Sweden
Tysland Hole	coke	lump	Electric	liquid	1937	Sweden, Norway
Wiberg	coke	pellet	Shaft	sponge	1952	Sweden
HyL I	nat.gas	pellet	Retort	sponge	1953	Mexico
Nu-Iron	nat.gas	fine	Fluidbed	powder	1962	USA
SL/RN	coal	lump	rot.kiln	sponge	1964	Canada
Midrex	nat gas	pellet	Shaft	sponge	1967	USA
Purofer	nat gas	pellet	Shaft	sponge	1970	Germany
Fastmet	coal fine	fine	RHF	sponge	1974	USA
HyL III	nat gas	pellet	Shaft	sponge	1980	Mexico
Iron Carbide	nat gas	fine	Fluidbed	fineFe_3C	1989	USA
COREX	coal	lump	Smelter	liquid	1989	Germany
INMETCO	coal fine	fine	RHF	sponge	-	Canada
CPR Pellet	coal fine	fine	RHF	sponge	developing	India

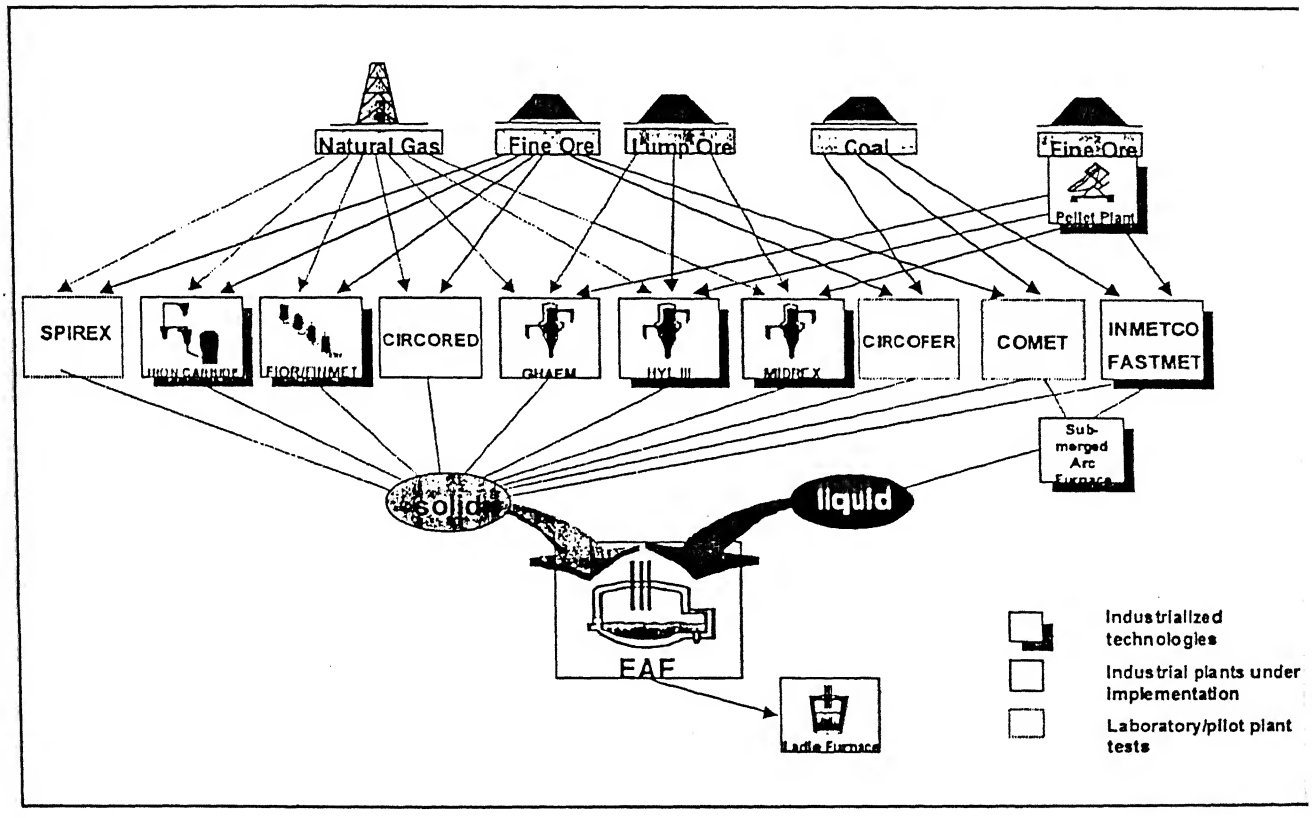

Fig. 2.2 : DR-technologies.[24]

$$CH_4(g) + \frac{1}{2}O_2(g) = CO(g) + 2H_2(g) \quad (2.1)$$

$$CH_4(g) + H_2O(g) = CO(g) + 3H_2(g) \quad (2.2)$$

Reactions (2.2) is preferred since it yields more H_2 than CO, and H_2 reduces iron oxide 5-10 times faster than CO. However, it is an endothermic reaction. Since reaction (2.1) is exothermic, both oxygen and steam are employed to make the process autogeneous. Nickel catalyst on ceramic substrate is typically employed to speed up reforming reactions. Midrex employs a continuous counter current, vertical gas-solid reactor, resembling more or less the stack of a normal blast furnace. Pellets or lump iron ore are fed into shaft from the top and the sponge iron, in cooled conditions, is removed from the bottom. The reducing gas is introduced from the bottom. The system consists of an efficient off-gas recovery and circulation unit, which makes it economic as well as environmental friendly.

Improved technology[4] coupled with increased operating experience has led to the development of larger direct reduction modules. Today, single-module Midrex plant are capable of producing in excess of 1.2 million tonnes annually, using a wide variety of iron oxide pallets and lump ores, and a range of energy sources. The energy required at the Portland Plant (U.S.A) is nearly 3.5 Giga cal per tonne of iron production and about 90 percent of this is met by using natural gas. Continuous nature of the process, efficient energy use, amenability to automation and control, as well as high degree of metallization (92-95%) and fairly high carbon content of sponge, have led to wide acceptance of Midrex process.

2.2.3 HYL Process

In this process sized iron ore is reduced by passing reformed natural gas, downwards through a static bed of sized ore or pellets. The reformed gas has approximately 75% H_2, 14% CO, 3% CH_4, and 8% CO_2. Reduction is carried out at 870-1050^0 C.

The pellets/ore in an individual reactor is processed in four stages :

(1) preheating and partial reduction of Fe_2O_3

(2) primary reduction to metallic iron

(3) cooling of the sponge iron by fresh, cold reducing gas

(4) discharging of DRI from the reactor and fresh charging.

There are four reactors (retorts). Each one is at a different stage at some time. Reducing gases are heated up in the reactor at stage 3, do primary reduction in reactor at stage 2, and go out through the reactor in stage 1 thus preheating and partially reducing the fresh charge.

The capacity can be increased either by increasing the individual size of the reactor or by multiplying the units into a battery of units. HYL has recently developed a direct reduction process[5] that does not require a reformer. It is called self-reforming process, where the reforming of the natural gas takes place in-situ inside the reduction reactor itself using the metallic iron of the DRI as catalyst. There is only one reactor and is continuous like Midrex. During normal operation of all reformers, actions must be taken to condition the feed gas in order to avoid carburisation or poisoning of the catalyst. In this case, since the catalyst (metallic iron) is continually renewed in the reduction zone,

neither the carburisation nor the poisoning of the catalyst represent any problem for the 'in-situ' reforming reactions.

The first industrial installation for a DR plant without the reformer started production in 1998 in Monterrey, Mexico. This plant produces highly metallised DRI with a high content of iron carbide. The plant has a capacity of 675000 tonnes of DRI per year. In addition to being the first to employ the 'in-situ' reforming, it also includes the pneumatic conveying of hot DRI directly from the bottom of the DRI reactor to the meltshop. The reduction system of this plant includes the DR reactor and the reduction circuit. The DR reactor is the typical HYL reactor consisting of two zones.

Oxygen is injected in order to have some partial combustion of the reducing gas to increase its temperature above 1020^0C. Adjusting the oxidants (CO_2 and H_2O) in the gases entering the reactor can easily control the degree of carburisation of the DRI.

2.2.4 : Rotary Kiln Processes

These processes have essentially been designed to carry out reduction using solid reductant like non-metallurgical coal. Both ore and coal are fed as lumps. Additional liquid or gaseous fuel may be burnt to generate the working temperatures. A long, slightly inclined to the horizontal, slowly rotating kiln is employed to carry out the reduction. The solid charge is fed from that end which is at a higher level. It travels under gravity aided by the rotating motion, through several temperature zones. The reduced charge comes out from the

other end of the kiln. It therefore passes through a continuous heating and cooling kiln without coming in contact with atmospheric air. Reduced and cooled product is screened and the oversize is subjected to magnetic separation to obtain clean sized sponge while the non-magnetic oversized portion as well as the undersize are recirculated. The feed charge can be either sized natural ore or pellets. It started with the original SL process to which the RN refinement system was added later and is now known as SL/RN process. There are other patented processes such as TISCO, OSIL etc. which differ in details from SL/RN.

2.2.5 : Fluidized Bed Processes

2.2.5.1 : Finmet Process

A schematic flowsheet of the FINMET process for the Hedlant plant in the Pilbara region of Western Australia is shown in Fig 2.3. The first processing step involves the removal of gangue from the ore fines in the beneficiation plant. Iron ore fines containing 62-63 percent total Fe (mostly in the form of hematite, Fe_2O_3) and processed by standard gravity and magnetic separation to yield a concentrate of ≥67 percent total Fe and approximately 2 percent (SiO_2 + Al_2O_3). This concentrate has a wide size range (approximately –6.3 mm to +10 μm). Buffer stockpiles exist between the beneficiation and HBI plants. Concentrate reclaimed from stockpile is fed into a fluid bed ore dryer where the ore is dried at 90-100^0 C prior to being charged to the feed system day bins.

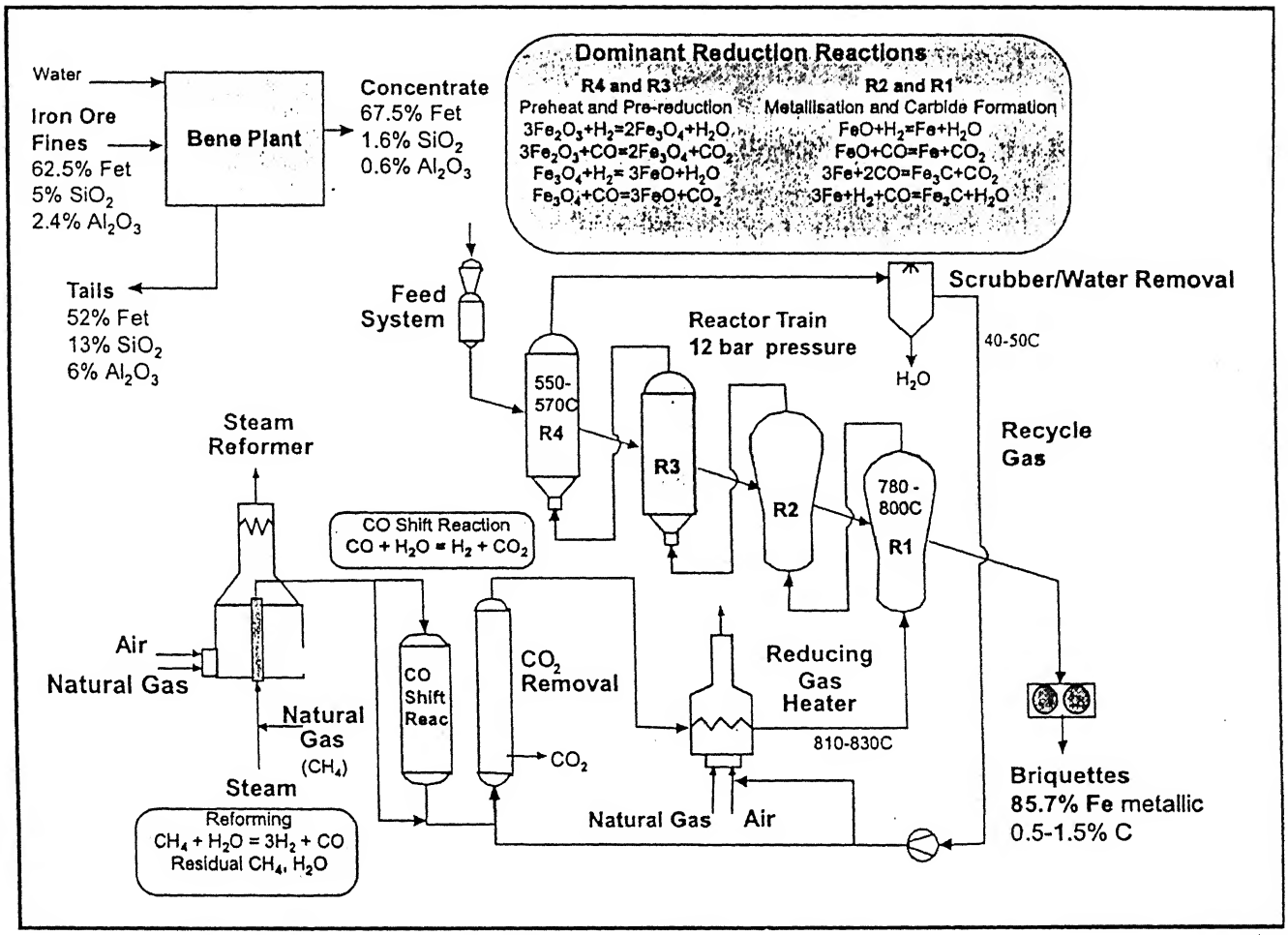

25

Fig. 2.3 : Schematic flowsheet of the FINMET process.

The FINMET process uses a train of four fluid bed reactors, with counter-current gas/solids contacting down the reactor train. Conditions within each fluid bed are maintained to ensure adequate solids mixing and efficient gas/solids contacting. The feed concentrate enters the topmost reactor (R4) where it is preheated to 550-570^0 C by reducing gas leaving reactor R3. Preheating is accompanied by ore dehydration, decrepitation and reduction of hematite to magnetite as shown in Fig 2.3. The beneficiated ore is transferred downward between reactors via standpipes and is progressively reduced first to FeO, and then finally to metallic Fe. The temperature in the bottom reactor (R1) is in the range of 780-800^0 C and finally reduction to 93 percent metallisation is accompanied by carburisation of some of the Fe to Fe_3C (iron carbide). The carbon content of the product can be varied by adjusting the composition of the recycle gas entering R1. The hot, fine DRI is then transported by a sealed, pneumatic lift system, or raiser, to the briquetter area where it is briquetted at temperature >650^0 C in a double roll briquetting machines to a density ≥5.0 g/cm^3. Fines separated out in the trommels are recycled to the briquetting press. The briquettes are then air cooled on a cooling conveyor and sent to product stockpile.

The reductant is reformed natural gas. There is elaborate arrangement to extract heat, remove H_2O, CO_2 from the off-gas and recycle the same. This is a standard feature of all established processes based on natural gas, such as Midrex and HYL. After its start-up in February, 1999, over 100,000 tonnes of HBI has been produced and sold in the market.

2.2.5.2 : Nu-Iron Process[6]

It is a process of manufacturing sponge iron by reduction of fines of iron ore in fluidized beds in reducing gas. The working conditions for Nu-iron process are Medium temperature, pure H_2 and medium pressure. Concentrates are reduced in the fluidized-bed reactor with pure H_2 at about 600 to 760^0 C.

The reducing medium is obtained from natural gas, coke-oven gas, or fuel oil by the following reaction stages :

Cracking with excess oxygen

$$CH_4(g) + \frac{1}{2}O_2(g) = CO + 2H_2(g) \qquad (2.1)$$

and conversion of the CO by excess steam

$$CO(g) + H_2O(g) = CO_2(g) + H_2(g) \qquad (2.3)$$

followed by removal of the H_2O and CO_2 in a hydraulic scrubber. There remains pure hydrogen which is brought up to the reactor input temperature of about 540^0 C by passage through a heat exchanger and a gas heater. The CO component, which would in itself have been usuable for the reduction, must be replaced as above by H_2. Since otherwise the Boudouard reaction would take place in the ore at 500^0 C and would thus disturb the reduction through the separation of carbon. Even with small bed heights, the gas utilization is close to the equilibrium value. The unused H_2 is recirculated after removal of H_2O. After the reduction is over the reduced ore is taken out of the fluidized reduction chamber and is briquetted for further processing.

Fig 2.4 shows the effect of temperature upon rate of reduction in Nu-iron process. At a temperature approximately below 600^0 C, the sponge iron is

is porous with a large pore surface area pyrophoric and difficult to handle. Rate is also low. At temperature above approximately 750^0 C, reduced metallic iron particles tend to grow by collision and sintering. As a result, the fluidized bed tends to get defluidized. Hence the operating range is 600-750^0 C.

2.2.5.3 : Circored and Circofer Processes[7]

Both these processes have been developed by Lurgi, Germany. Circored is gas based and Circofer is coal based. These employ one two-stage circulating fluidized bed (CFB) and one fluidized bed (FB) reactor. Rate of reduction is very fast upto 65 to 75 percent degree of reduction and then it considerably slows down for iron oxide fines. Therefore for initial stages CFB offers advantages due to high gas velocities and rapid heat and mass transfer rates. For further reduction, bubbling FB reactor is better since gas velocities are low and retention times are high. Fig 2.5 shows the velocity and other characteristics of different types of reactors.

In Circored process, hydrogen obtained from natural gas reforming or from any other source is used as the single reductant. As it is known that the commonly used iron ore fines do not display a sticking tendency at reduction temperatures <650^0 C, hence a low operating temperature was selected for CFB reactor. The finally reduced fines discharged from FB reactor is at a temperature of 630-680^0 C. these are then heated to 700-730^0 C for making of HBI.

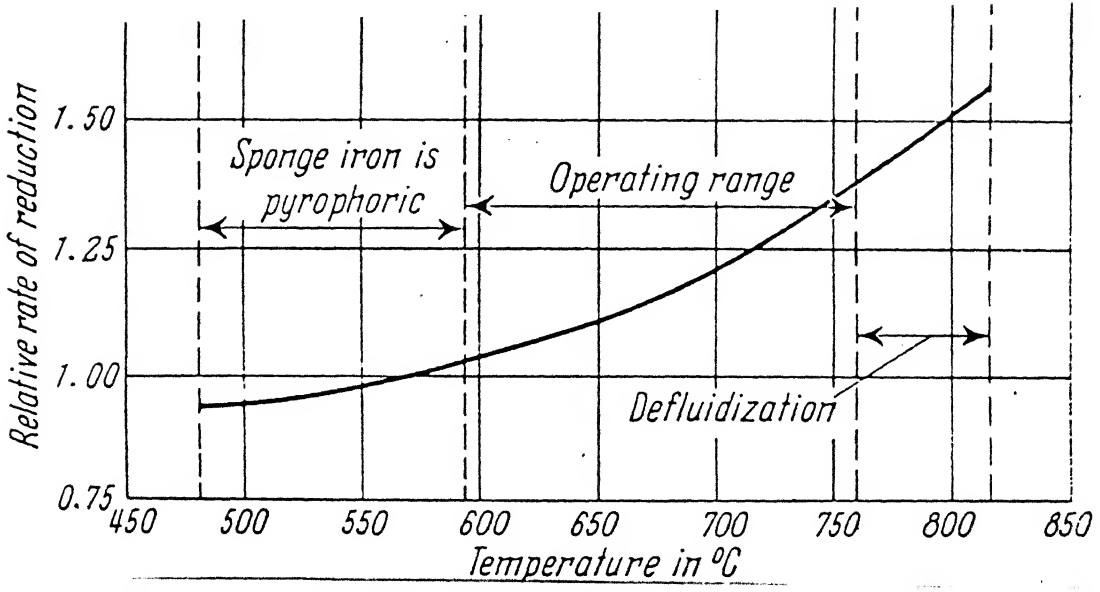

Fig. 2.4 : Effect of temperature upon rate of reduction in Nu-iron process.[6]

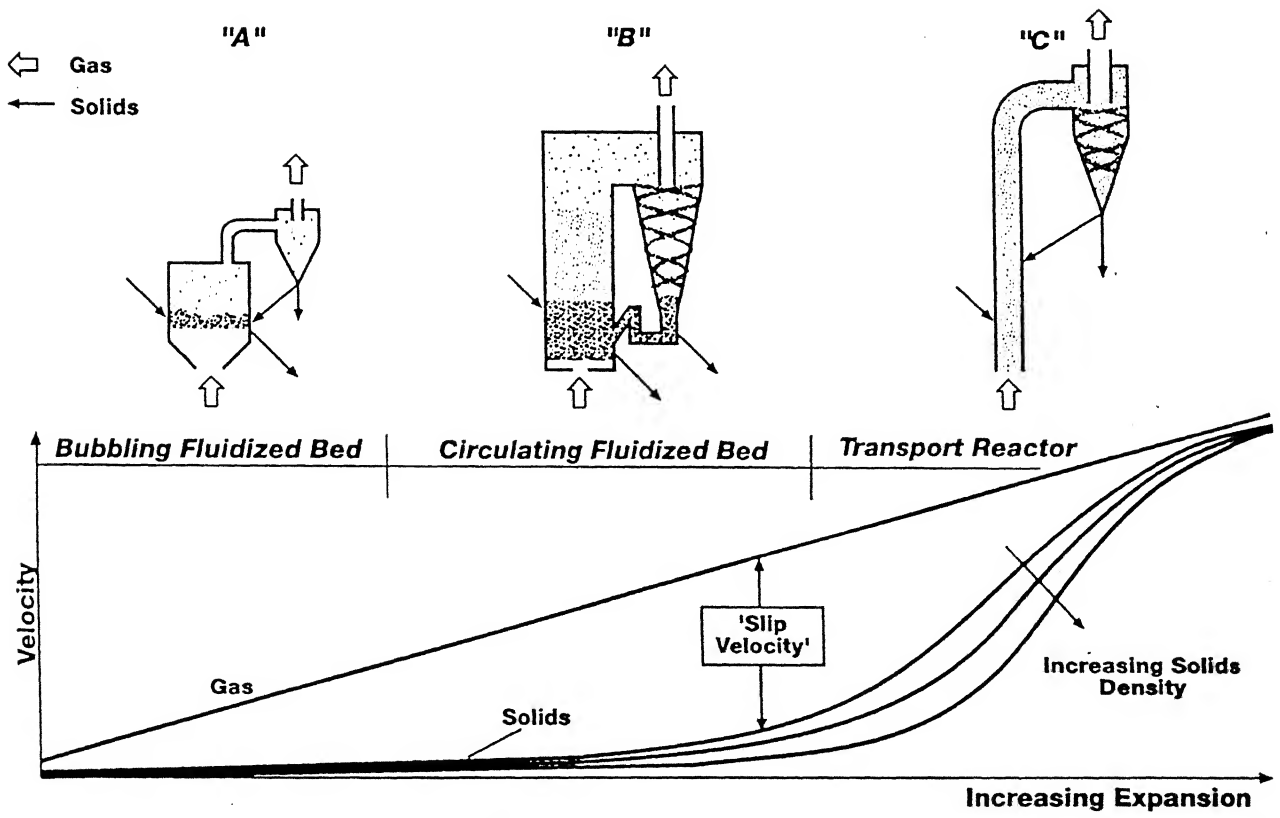

Fig. 2.5 : Fluidised bed systems.[26]

In the Circofer process, coal fines are partially oxidized in an external unit to give a product which is mixture of char, CO gas at a temperature of approximately 1000^0 C. This mixture along with iron ore fines are processed in CFB and FB at a temperature of 850-950^0 C. The FB reactor discharge is cooled below the Curie point of iron and then subjected to magnetic separation. The iron is pressed into HBI, the char is recycled. Sticking of reduced iron particles is prevented due to presence of large quantities of char fines (about 10 times) in the fluidized bed. The developments are in pilot plant stage.

2.3 : Smelting Reduction (SR) Processes of Iron-making

Metallurgical coking coal is costly and reserves are coming down. Also coke ovens are a source of environmental pollution. Either they have to be made environmental friendly or have to be closed down. Therefore iron and steel industries throughout the World seriously started exploring the possibility of making liquid iron directly using non-coking coal. In the last two decades, some processes have been developed. A common feature of these is that they require pure oxygen for favourable heat balance. Most recent source of these processes is the proceedings of the International Conference on Alternative Routes of Iron and Steel making held on 15-17 September 1999, Perth Australia. Another valuable source is the International Conference on Alternative Routes to Iron and Steel, held at Jamshedpur in 1996.

The first commercially successful process is the COREX process, developed and marketed by VOEST-ALPINE Industries, Austria (VAI). Fig (2.6) shows a flow sheet of the process. It employs lump ore or pellets, or mixture thereof, as raw materials. It is a two-stage process. In the reduction shaft, the ore is reduced upto 93 percent by a reduction gas moving in counter current. Discharge screws convey the DRI from the reduction shaft into the melter gasifier where final reduction and melting take place in addition to all other metallurgical reactions. Tapping of hot metal and slag is then carried out as in the conventional blast furnace practice.

Non-metallurgical coal is charged directly into the melter gasifier. Combustion with oxygen injected into the bath results in the generation of a highly reducing gas. Volatile matters of coal also get dissociated into CO and H_2 because of high temperature. The dust coming out with exit gas is separated by a hot cyclone. The top gas is subsequently cooled and cleaned in a scrubber and is available as valuable export gas for other uses. A commercial COREX unit has been commissioned in South Africa and recently in Karnataka in Jindal Vijaynagar Steel Ltd. Another plant is under commissioning in South Korea.

Two parameters[8-9] have received wide attention in connection with SR processes. These are :

(a) Post-combustion ratio (PCR), defined as

$$\text{PCR (express in pct.)} = \frac{CO_2 + H_2O}{CO_2 + H_2O + CO + H_2} \times 100 \qquad (2.4)$$

Where CO_2 etc. denote fraction CO_2 etc. in the outgoing gas from the smelter reactor.

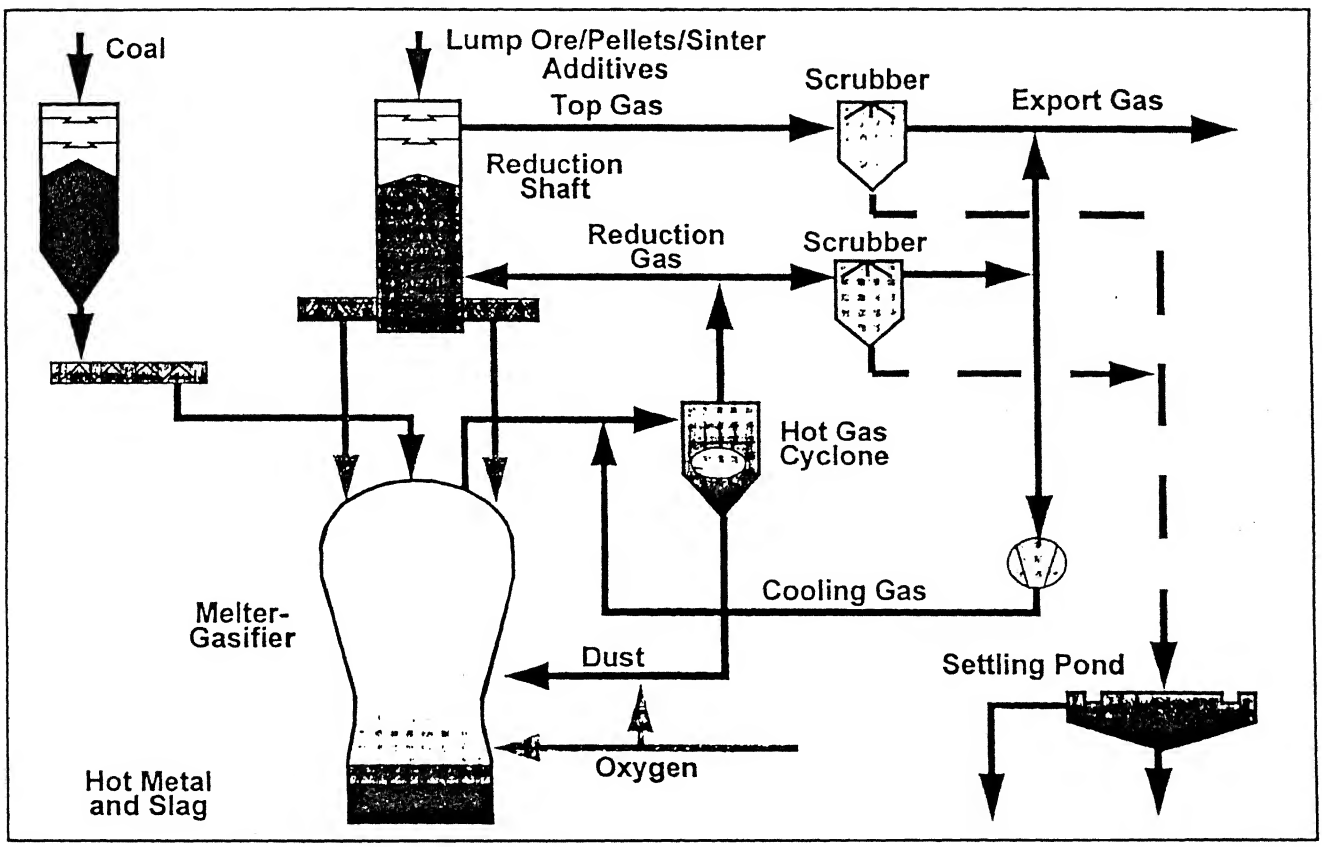

Fig. 2.6 : Flowsheet of the COREX process.[24]

(b) heat transfer effeciency (HTE), defined as :

$$\text{HTE (expressed in pct)} = \left[1 - \frac{H_{Tg} - H_{Tb}}{\Delta H_{PC}}\right] \times 100 \qquad (2.5)$$

Where H_{Tg} = enthalpy of exit gas at exit temperature

H_{Tb} = enthalpy of exit gas at bath temperature

ΔH_{PC} = heat generated by post-combustion reactions.

PCR is a measure of combustion of CO and H_2 to CO_2 and H_2O by oxygen/air in slag layer and above slag layer. High PCR leads to utilization of fuel value of CO and H_2 more in the smelting reactor itself. Hence it lowers coal consumption.

For fuel efficiency it is also necessary that the heat generated in the post combustion is transferred to slag and metal to sustain endothermic reactions there and counter heat losses. This requires a high HTE. In COREX process PCR is less than 10 percent. Hence if heat of exothermic reaction of coal is not properly utilised in power generation or in some other unit, economy suffers. The second generation processes developed later, such as HISMELT, DIOS, AISI, have gone for PCR above 50 percent and the coal consumption has come down to 600-700 Kg/tHM. Utilisation of this heat also has been possible since HTE for these processes is above 80 percent.

Table 2.6 provides a brief overview of the various SR processes[17]. These processes can be classified into single stage, two stage and three stage processes, as illustrated in Fig 2.7. The essential classification of SR processes according to some of these considerations is presented in Table 2.7. Fig 2.8 shows the status and raw materials usage of these processes.

Table 2.6 : An overview of selected SR processes[17]

Process	Type of Reactor	Reductant/Energy	Oxide feed	Product	Application	Status
COREX	Shaft reduction and gasifier	Coal, oxygen	Lump ore, Sinter, Pellets	Hot metal	Steelmaking	0.3 Mtpa commercial plant. 0.6 Mtpa unit under commissioning.
ROMELT	Rectangular smelting reactor	Coal, oxygen, electricity	Iron ore	"	"	0.3 Mtpa plant operational
HISMELT	Fluidised bed reactor, horizontal converter or melter	Coal, oxygen, electricity	Ore fines	"	"	0.1 Mtpa plant under commissioning
DIOS	Fluidised bed pre-reduction furnace, gas reforming furnace and iron bath SR furnace	Coal, oxygen, electricity	Ore fines	"	"	Pilot plant (50 tpd) started in 1993.
AISI	Pre-reduction shaft and iron bath smelter	Coal, oxygen, electricity	Ore fines, Pellets	Semi steel	"	Pilot plant trials completed in August 1994, presently no activities reported. Utilisation of steel plant wastes to be tried in the next phase.
ELRED	Fluidised bed reactor, D.C. EAF	Coal & Coke, electricity	Ore fines	Hot metal	"	Pilot plant started in 1976, now abandoned.
INRED	Flash smelter and electric smelting furnace	Coal, oxygen, electricity	Ore fines	Hot metal	Steelmaking	Pilot plant started in 1980, limited trials, now abandoned.
PLASMA-SMELT	Fluidised bed for pre-reduction and SR in shaft with plasma generator	Coal, coke, electricity	Dried iron ore concentrate	"	"	Pilot plant started in 1982, no activity reported recently.
SUMITO-MO SC	Reduction in shaft type furnace and melting gasification furnace	Powdered coal, oxygen, steam	Ore/Pellets	"	"	Pilot plant in 1982, no activity reported recently.
AUSMELT	Converter with top submerged lance	Lump and powdered coal, oxygen, air	Lump/ fines	Pig iron, Fe-Ni	Steelmaking/ Fe-Ni production	Well estabilished technology in non-ferrous extraction, pilot plant for pig iron production

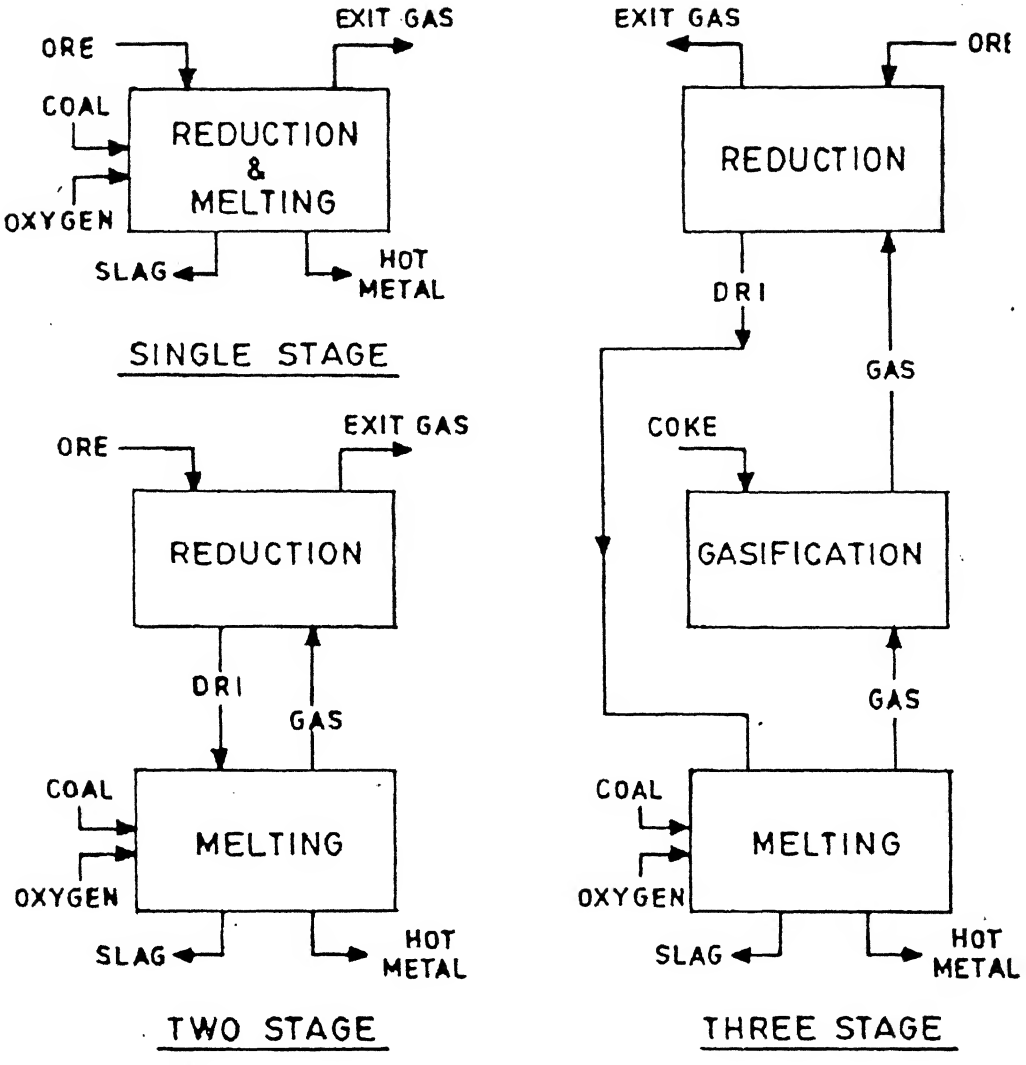

Fig. 2.7 : Flowsheet for smelting reduction processes.[23]

Table 2.7 : Classification of SR Process.[29]

Criterion	Class	Major Processes Under the class	Remarks
A) According to level of PCD*	a) Processes with high (more than 30%)	-Romelt, Hismelt, DIOS, AISI	
	b) Processes with low PCD (less than 10%)	-Corex	
B) According to usage of oxygen or air	a) Processes using oxygen alone with little or no air	-Corex	
	b) Processes using air alone with little or no oxygen	-Hismelt	
	c) Processes using air and oxygen in combination	-Romelt	
C) According to usage of electricity as energy source	a) Processes using electricity as energy source	-Inred, Elred, Plasmasmelt -Combismelt.	
	b) Processes not using electricity as energy source	-Corex, Romelt, Hismelt DIOS, AISI	
D) According to number of reactors used	a) Single reactor process	-Romelt	Process developers of DIOS have kept their options open whether they would use two or three reactors.
	b) Two reactors process	-Corex, Hismelt	
	c) Three reactors process	-DIOS	
E) According to number of "stages or "Reaction Zones" employed	a) One stage process	-Romelt	
	b) Two stage process	-Hismelt, DIOS, AISI	
	c) Three stage process	-Corex, DIOS	

* Post Combustion Degree (PCD) is defined as :

$$PCD=(\%CO_2+\%H_2O)/(\%CO+\%H_2+\%CO_2+\%H_2O)$$

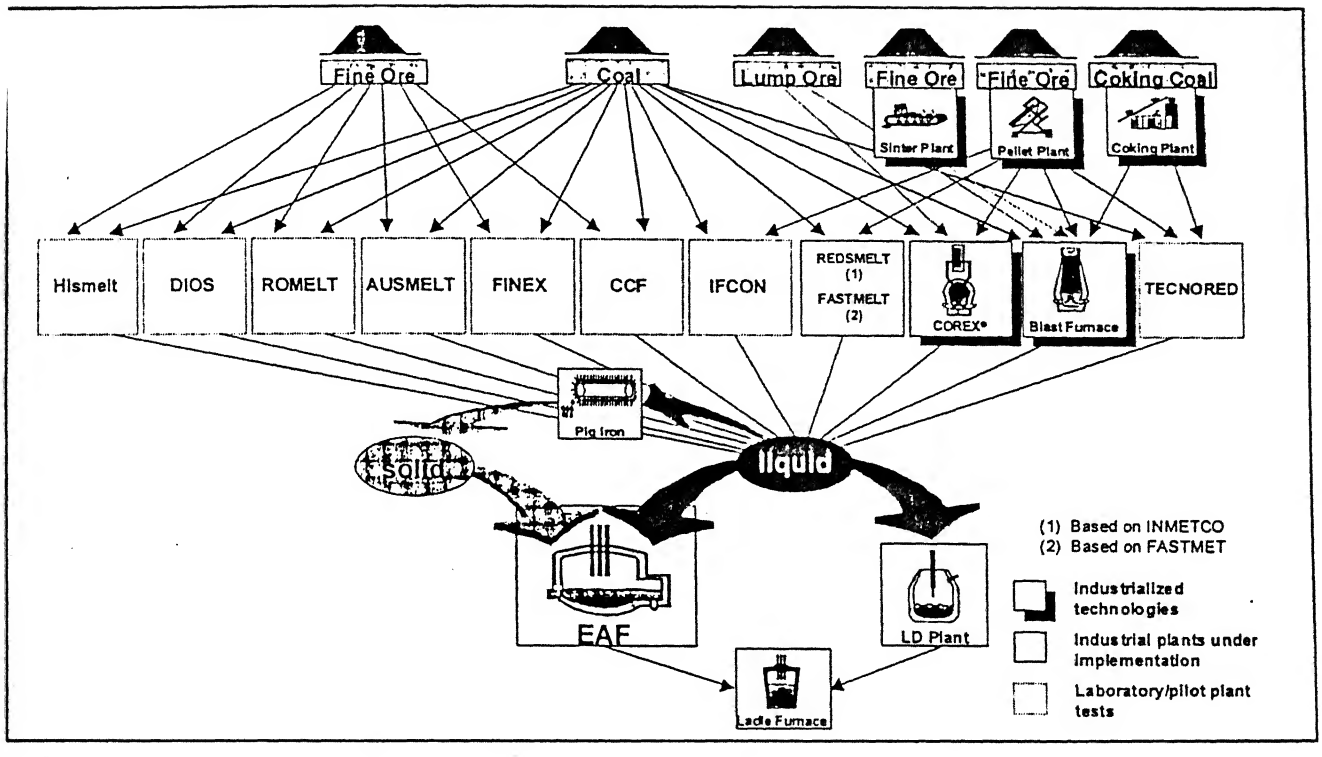

Fig. 2.8 : SR-technologies.[24]

This process is being seriously considered by integrated steel plants in India for further development and adaptation[10].

In the erstwhile USSR, the development of liquid-phase iron reduction process was initiated by Moscow Institute of Steel and Alloys (MISA) in late 1970s. In contrast to other known processes, it is a single-stage bath smelting process. It has been named as 'ROMELT' process, and has been operated in pilot plant scale in Russia. Liquid iron is produced in a molten slag bath reactor using non coking coal and oxygen. Post combustion of the primary bath gases and transferring the major part of the resultant heat back to the bath are the principal driving force of the process.

For a single stage process like ROMELT, a PCR above 70 percent with high HTE would be required. Oxygen is introduced in the reactor at two different levels through water cooled tuyers. The lower level tuyers are submerged in the slag and provide oxygen enriched air blast (40-60 percent) for gasification of carbon and bath agitation, while upper rows of tuyeres supply pure oxygen (95-99 percent) there by achieving high degree of post combustion of gases (60-70 percent).

Main advantages claimed for the ROMELT processes are :

(a) Single stage smelting reduction process directly using iron bearing materials and non coking coal for production of liquid iron

(b) minimum preparation of raw materials -no limitations on size range or moisture content

(c) flexibility in use of wide range of iron bearing materials include lump ore, ore fines, sinter, pellets, ferrogenous wastes generated in the steel plant including sludge either individually or in any combination.

The coal quantity should be proper for use in SR processes. It should have low ash, low volatile. Fig 2.9 shows the quality of coal usable in COREX which is roughly true for other SR processes. Most of the Indian non-coking coals are high in ash and VM and, hence unsuitable for use unless these are blended with good quality coal. Bhattacharya etal[11]. Have carried out comparision of COREX and ROMELT including financial analysis in the Indian context. Production cost and other key financial parameters are comparable.

2.3.2 : Some fundamental considerations of smelting reduction

Here we shall briefly review some fundamental aspects, of only SR. Earlier the two fundamental parameters, viz. post combustion ratio and heat transfer efficiency have been presented and their importance in development of second generation SR processes has been mentioned. Koria[12] has developed a thermochemical model to study the two stage smelting reduction process without post combustion. Hence it is valid only for COREX which has a very low PCR. The model was applied to commercial data for a COREX plant, and reasonable agreements have been reported. A 4 percent increase in metallization was found to decrease the coal rate by 5 percent and also influence other parameters. At a given percent metallization, the coal rate and export gas were found to be lowest for anthracite as compared to all other types of coal.

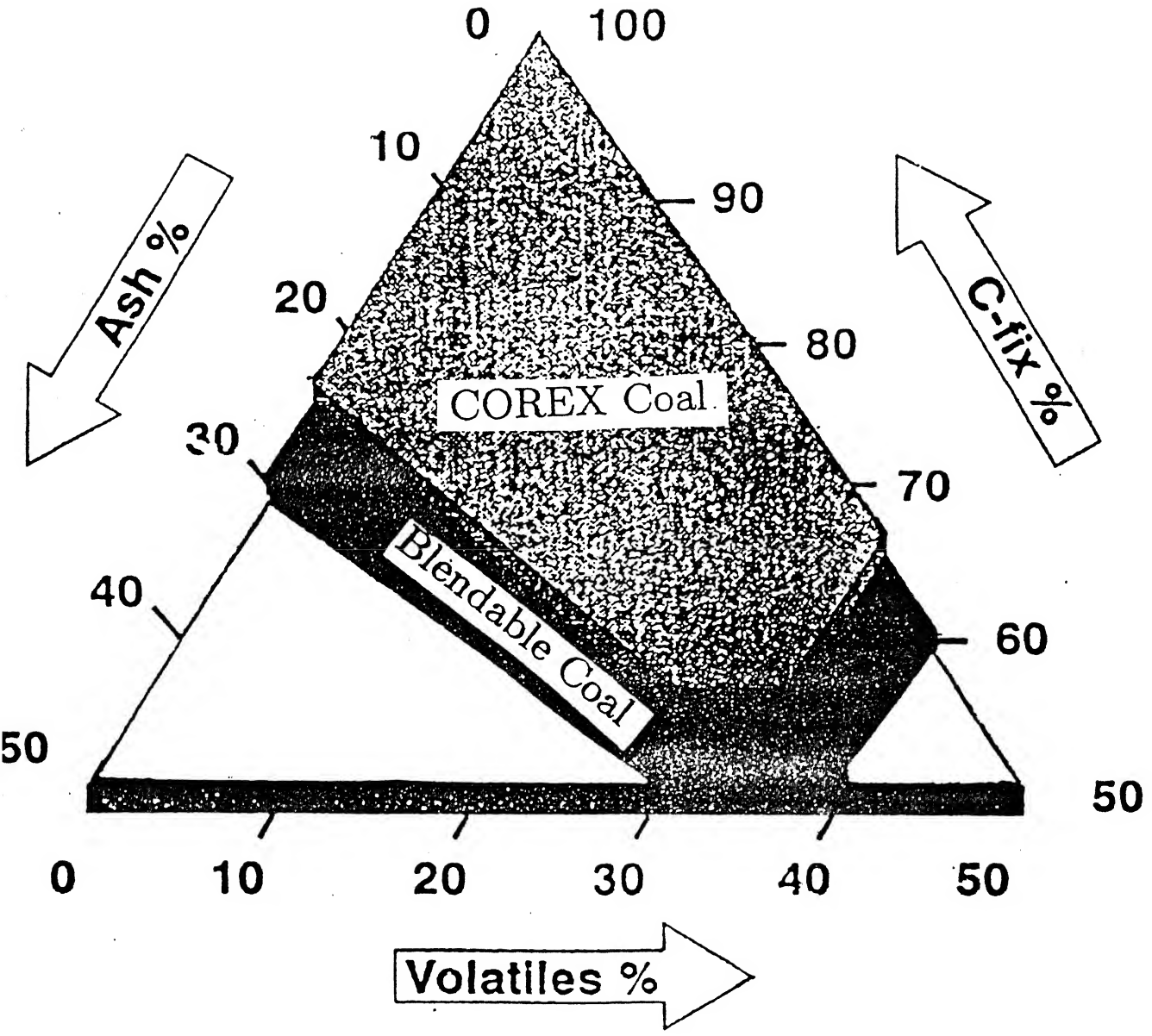

Fig. 2.9 : Usable coals for COREX.[27]

Ghosh[13] has analysed fundamentals of productivity of smelting reduction processes, consisting of two stages viz. prereduction (PR) and smelting reduction (SR). Productivity of shaft type PR unit is expected to be limited by rate of reduction of iron ore, and hence would be governed by the reduction characteristics of the ore by gases. Productivity of circulating fluidized bed PR units is more difficult to estimate theoretically. Productivity of an SR unit is limited by slag foaming and reduction of FeO dissolved in slag by carbon. PCR is currently less than 5 tonnes/day/m^3. So far as melting reactor is concerned, Fig 2.10 shows bath smelting schematically. Due to gas generation and evolution, the slag foams extensively and metal droplets are ejected into the slag as droplet forming a slag-metal-gas emulsion. In addition of these char particles also are dispersed into the slag.

Here we are primarily concerned with reduction of FeO dissolved in slag by carbon. Large number of fundamental kinetic studies have been carried out on this system. The overall reaction is :

$$(FeO)_{\text{in slag}} + C_{(s)} \text{ or } [C]_{\text{in liquid Fe}} = [Fe] + Co_{(g)} \qquad (2.6)$$

There is general agreement that it occurs in 2-stages, viz.,

Slag-gas reaction :

$$(FeO) + CO(g) = [Fe] + CO_2(g) \qquad (2.7)$$

carbon-gas reaction :

$$C + CO_2(g) = 2CO(g) \qquad (2.8)$$

The overall reaction is endothermic. The process is complex. At least three phases would be present. Extensive emulsion formation and consequent

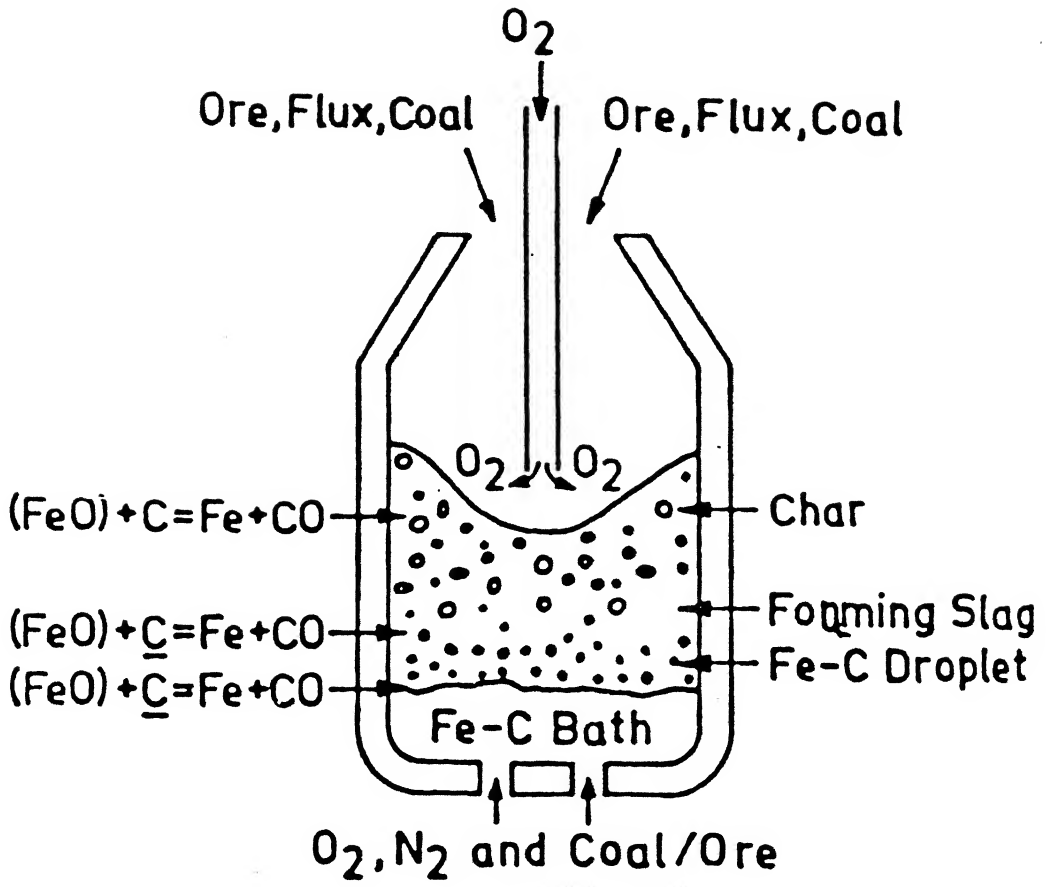

Fig. 2.10 : Schematic diagram of Bath Smelting.[14]

dispersion of phase make reaction geometry complex and interfacial areas unknown. An interesting feature is :

Faster reaction → more vigorous gas evolution → more intense stirring and larger interfacial area → enhancement of rate.

Rate of reaction $(r) \propto (W_{FeO})^n$ (2.9)

Where $1<n<2.5$. (W_{FeO}) denotes weight percent FeO in slag. Value of $n>1$ has been explained by the autocatalytic nature of the reaction as noted above.

Fruehan and coworkers[14] attempted to estimate productivity of smelting reactors as follows :

Rate of production∝rate of reduction∝rate of gas generation (2.10)

Again, foam volume∝foam height∝rate of gas generation (2.11)

Foam height was calculated from the following equation :

$$\text{Log}(\Pi_1) = 5.11\text{-}2\log(\Pi_2) \quad (2.12)$$

Π_1 and Π_2 are dimensionless numbers and,

where, $\Pi_1 = \sum \frac{\mu_g}{\sigma}$ and $\Pi_2 = \frac{P\sigma^3}{g\mu^4}$ (2.13)

Here P is productivity

σ is surface tension of slag

μ is viscosity of the liquid

μ_g is viscosity of gas and

g is accelaration due to gravity.

Again, volume available for foaming (V_A) is given as :

$$V_A = V_T - V_S - V_M \quad (2.14)$$

Where V_T is total reactor volume, V_s and V_M are volumes of slag and metal respectively. Considering the following equation :

$$r = (K_{SM} A_B + K_{SC} A_C + K_{SM} A_D)(W_{FeO}) \quad (2.15)$$

where r is the total rate of reduction of FeO in slag, and K_{SM} and K_{SC} are the experimental rate constantsfor the slag–metal and slag–char reactions. A_B, A_C, A_D are bath area, char area and metal droplet area respectively.

Neglecting bath-slag reaction in Eq.(2.15) and taking A_C and A_D as proportional to slag volume, $r \propto V_S$. In other words, V_A decreases as rate of production increases. The limiting production rate, therefore, would be obtained when V_A becomes equal to increase in volume of slag due to foaming. This is shown schematically in Fig 2.11. Based on this approach Fruehan concluded that a productivity upto 10 t/d/m^3 is achievable at 1 atm. pressure.

In the second generation process the off gas from the smelter has high percentage of CO_2 and H_2O. Hence it is not able to reduce FeO into Fe in the prereduction unit. This limits the maximum productivity of current smelting reactor to about 8 t/d/m^3. Through a preliminary analysis Ghosh[15] has demonstrated that use of composite ore reductant pellet has the potential to increase productivity by about 50 percent.

2.4 : Concluding remarks

Another recent development for production of liquid iron is miniblast furnace. A conventional blast furnace has minimum volume of 350 m^3. Miniblast furnaces (MBF) have volume upto 300 m^3. Recently countries like

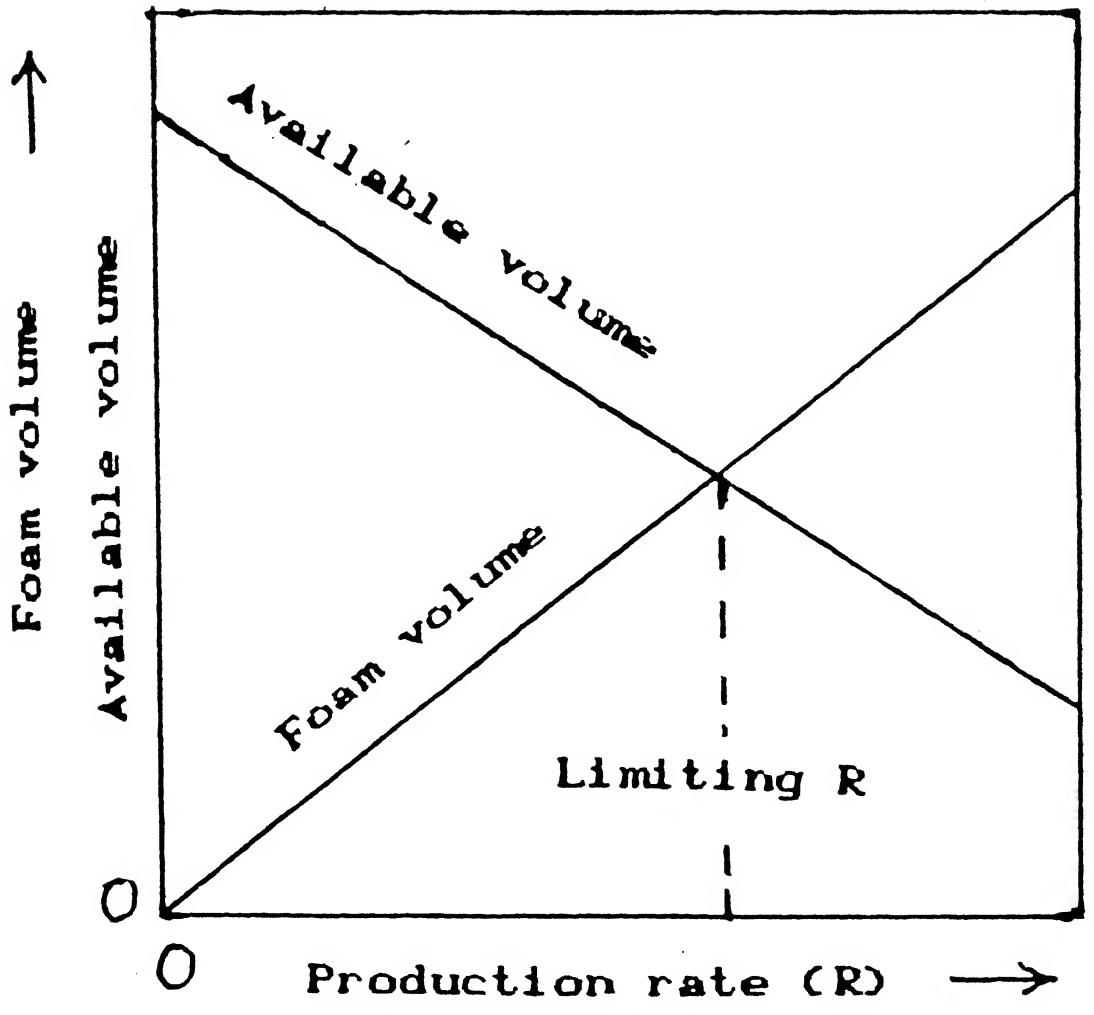

Fig. 2.11 : Foam and available Volume vs. Production rate in SR (Schematic).[14]

India and Brazil have commissioned a number of these MBFs[16]. As a matter of fact in India they are producing more than 1 million tonne per year. China played a pioneering role in developing technology of MBF. In a sense these are not alternative processes to blast furnaces. The basic driving force for growth of these have been the smaller capital requirement as compared to conventional blast furnaces.

As mentioned in chapter 1 that iron making via. The composite ore reductant route, such as FASTMET, FASTMELT processes, has considerable future potential. The present study is a fundamental one, relevant to this development. However, since these processes have been reviewed elsewhere[1], it will not be repeated here.

Chapter 3

EXPERIMENTAL PROCEDURE AND APPARATUS

3.1 : Trials with pellet making

The process of making pellets consisted of iron ore fines, activated char, and small amount of water without using any binding material. Since the study is fundamental in nature, it was decided to avoid the use of any organic binder as it would make the system complex. Various methods were tried out to make pellets having sufficient strength, which would not crumble during handling or after reduction, since these would lead to erroneous results.

In the first trial iron ore fines were mixed with activated char and a little quantity of water. The resulting mixture was subjected to a compaction pressure of 7.7 Kg/mm^2 and 10.8 Kg/mm^2 for one minute. The pellets were then oven dried at 100^0 C for 2-3 hours. After oven drying it was found that the pellets crumbled out.

In the second trial it was decided to repeat the same procedure as the earlier one, by adding a little bit of more water and leaving the pellet for two minutes in the machine. The pellets were then subjected to oven drying for five hours in stages at temperatures of 50^0 C, 100^0 C and 150^0 C respectively. It was seen that the pellets crumbled during handling.

In the third trial it was decided to add 2 percent bentonite as binder along with water, and the same procedure as in second trial was repeated. It was

found that still the pellets did not achieve the desired strength. It was also decided not to use too high compaction pressure to make the pellets because the product gases coming out after reduction may cause crumbling of the pellet, thus destroying its integrity. Hence it was decided to make pellets with mixture of iron ore fines and activated char in a stainless steel crucible and compact it in a pellet making unit as shown in Fig.3.1. The crucible containing the mixture was placed on a platform, and a mandrel was then placed just above the crucible supported by hand. An impact load of 0.45 Kg was then unscrewed from a height of nearly 13 cm and allowed to fall on the mandrel. This resulted in formation of a compact mass of cylindrical pellet.

3.2 : Raw materials preparation and characterization

3.2.1 : Size

The main aim was to carry out experiments with raw materials (blue dust and activated char) of −100 mesh size. Sieve analysis of blue dust and activated char was done with sieves of BSS mesh sizes 100, 200, and 240 with opening sizes of 152 μm, 76 μm, and 66 μm respectively. The results are presented in Table 3.1.

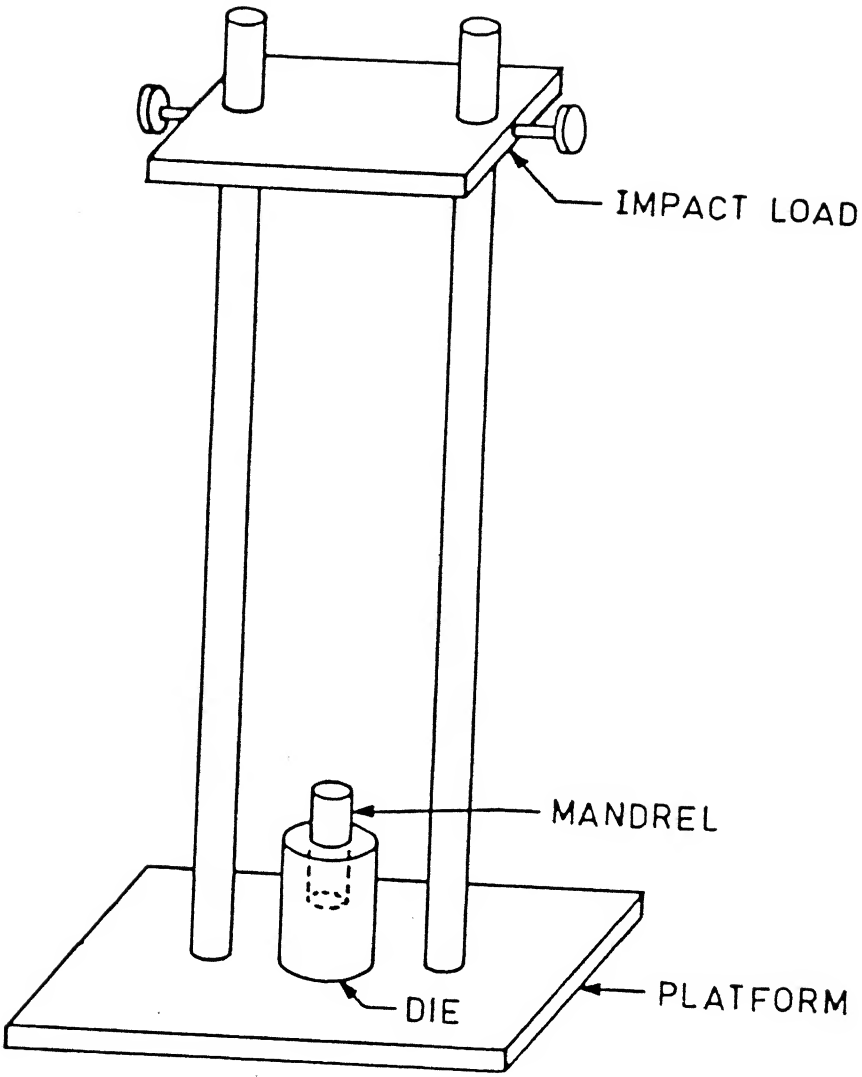

Fig 3.1 : Pellet Making Unit

Table 3.1

Size analysis of blue dust and activated char

Mesh size	Blue dust (%)	Activated char (%)
-100 + 200	72.49	45.21
-200 +230	25.33	54.78
-230	2.16	0.00

3.2.2 : Chemical characteristics

The blue dust used in this study has earlier been used by Dutta[18]. He carried out analysis of the blue dust by two different methods. The two methods were by (a) chemical analysis, and (b) by hydrogen reduction. The latter gave data on removable oxygen associated with Fe_2O_3. The results of his analysis are presented in Table 3.2. Proximate analysis of activated char was carried out to determine the volatile matter (VM) and ash content by following the standard procedure for their determination. It was found that the VM was 6.38 percent.

For the present study, since the solid reductant should be only carbon it was intended to reduce the volatile matter content. For this purpose an alumina crucible having internal diameter of 5.5 cm, and 12.5 cm as height with a graphite cover was used. The crucible containing 25 gm of activated char along with the graphite cover was kept in the muffle furnace at a temperature of 600^0 C for 45 minutes. Then the crucible was kept for another 1 hour in the furnace and the temperature was slowly raised from 600^0 C to 800^0 C. The alumina crucible was then taken out, cooled and further measurements were carried out.

The data obtained is as follows :

Fixed carbon – 91.78%

VM - 6.38%

Ash - 1.84%

Moisture - 0.00%

Table 3.2

Analysis of blue dust [18]

Total Fe (%)	Av*	Total Removable Oxygen (%)	Av*	Fe_2O_3 (pct) (By Chem Analysis)	(By H_2 Red)	Av*	Moisture (%)	Av*	LOI (%)	Av*
66.7		28.6					0.07		0.70	
	66.5		28.8	95.1	95.7	95.4		0.07		0.72
66.3		29.0					0.07		0.73	

Fe^{2+} = negligible, SiO_2 = 1.6 pct, Al_2O_3 =1.8 pct

Av* = Average, LOI = Loss on ignition

3.2.3 : Method of mixing and handling

In order to avoid erroneous results, adequate care was taken during mixing and handling of the mixture. If proper care is not taken, it may lead to segregation due to the difference in densities of iron ore fines and activated char. Hence in order to avoid this the following procedure was adopted.

The mixture of iron ore and activated char was kept in a bottle and mixed thoroughly by rolling the bottle in hand. Shaking was avoided in order to prevent segregation. The process of rolling was continued for 20 minutes to ensure that a homogeneous mixture is obtained. Finally before making pellet the bottle was again rolled for 5 minutes. Before using the mixture, the bottle was carefully taken out from the dessicator without giving any jerk to avoid segregation.

3.3 : Apparatus for reduction experiments

3.3.1 : Furnace

The reduction experiments were carried out in a horizontal tube furnace as shown in Fig 3.2. At one end the furnace head was connected with the inlet gas tube i.e., the tube through which the gases such as Ar, H_2, CO_2, are introduced into the furnace. At the other end through which the crucibles were introduced, the furnace head was connected with a bubbler to avoid any entry of air into the furnace. Temperature of the hot zone was measured by a chromel-alumel thermocouple. Fig 3.3 shows the temperature profile along the axis of the furnace.

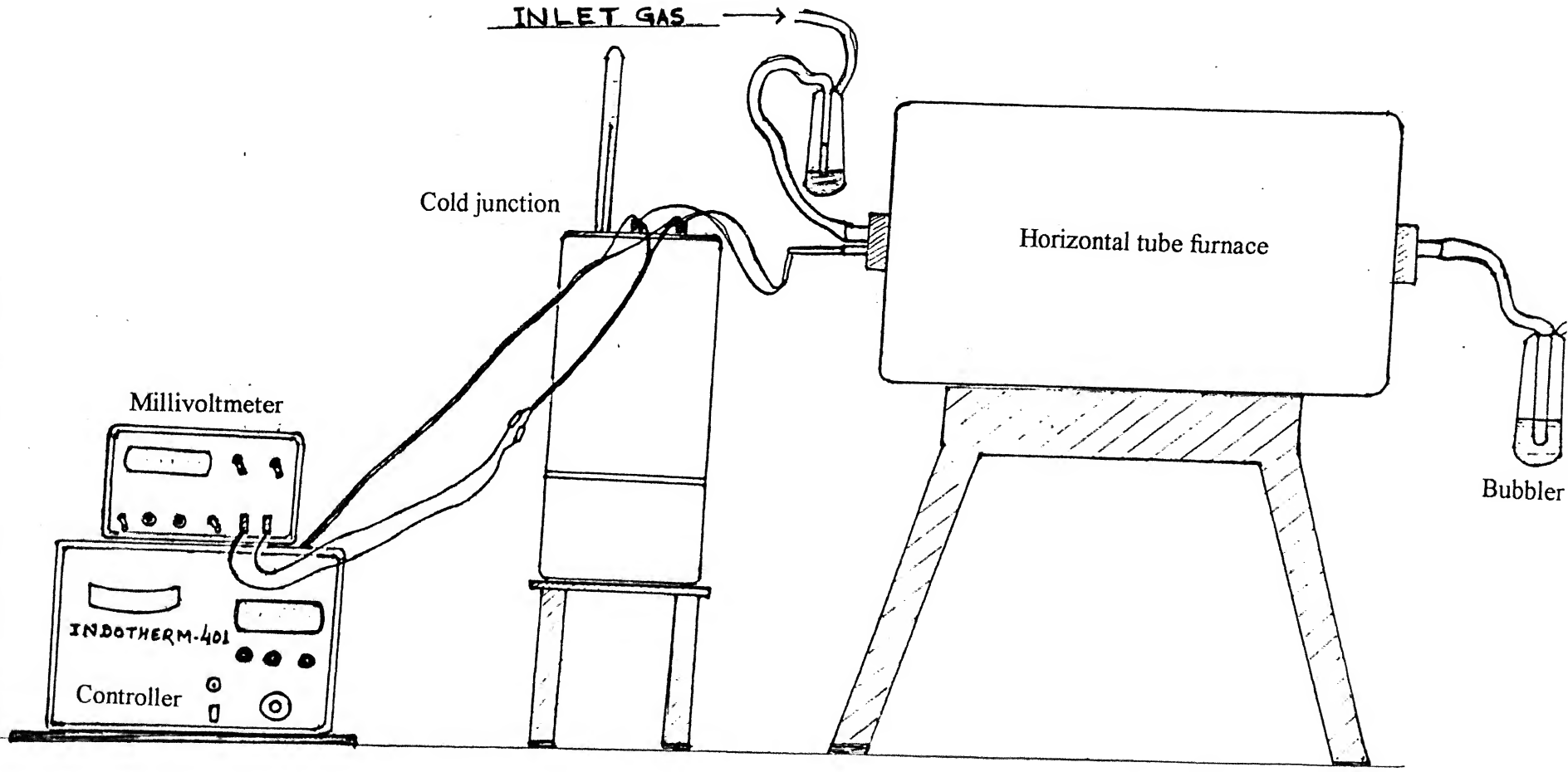

Fig 3.2 : Horizontal Tube Furnace

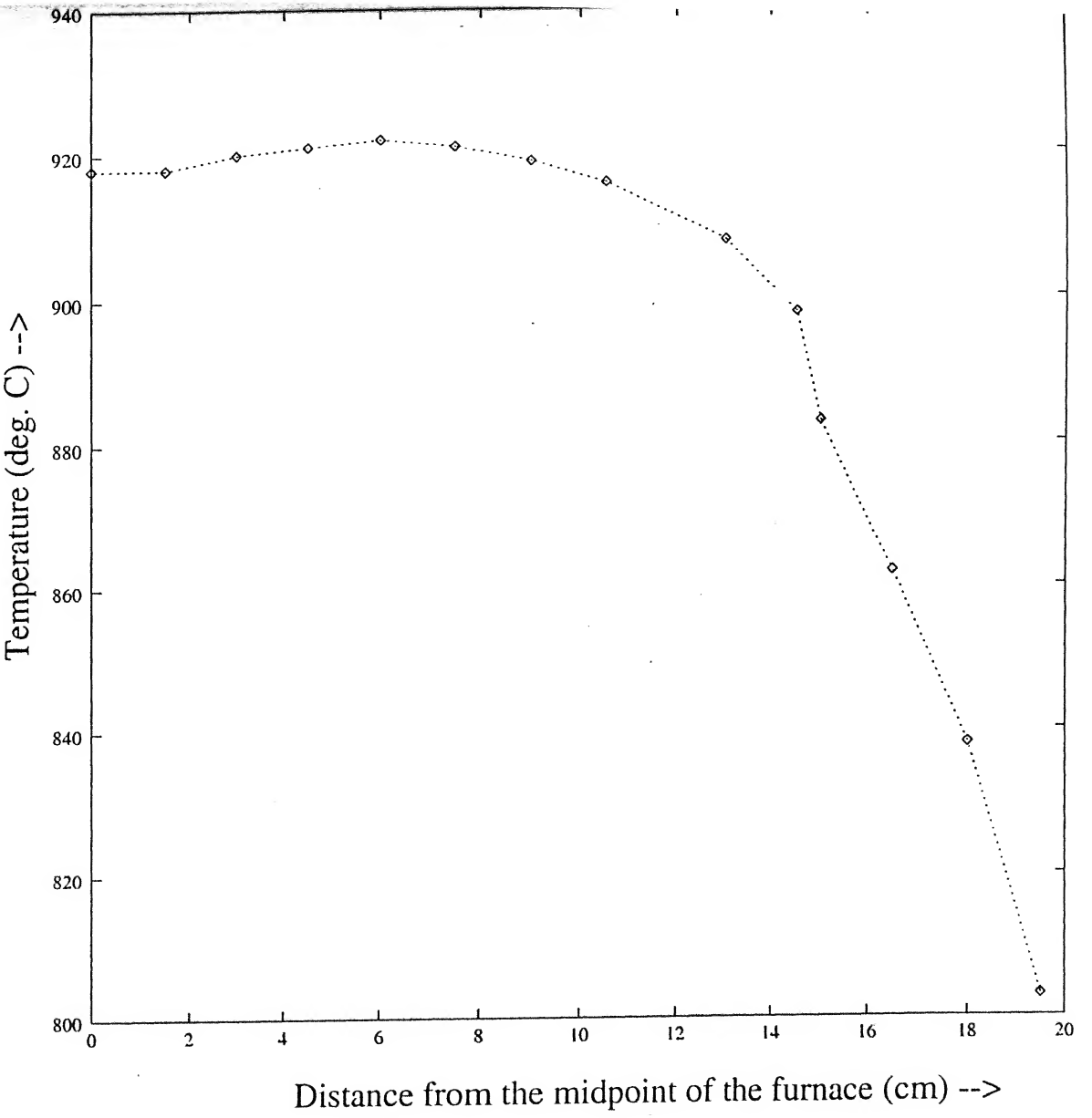

Fig. 3.3 : Temperature profile of the horizontal furnace

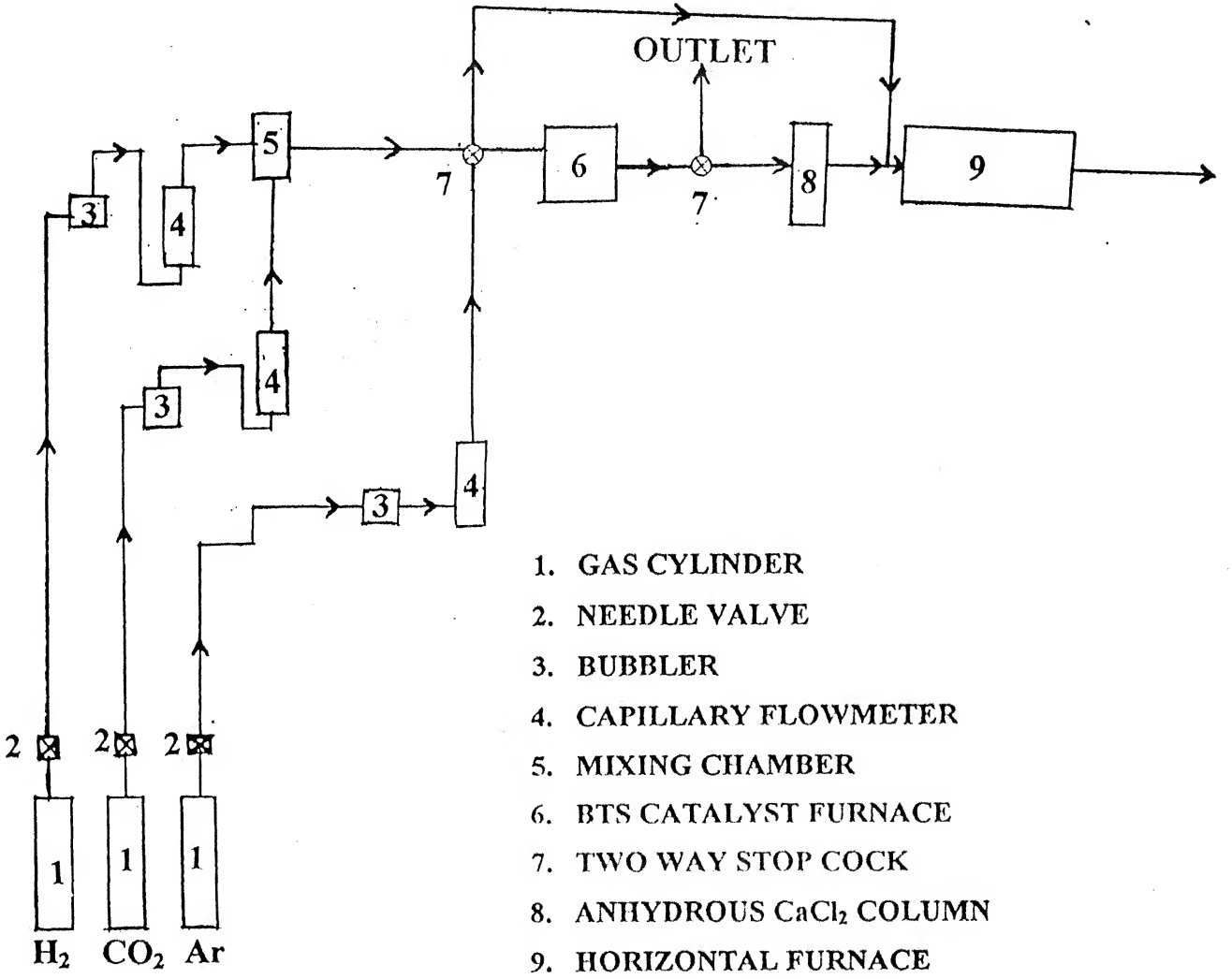

Fig 3.4 : Gas Train

The mullite tube, which was placed inside the furnace, had internal diameter of 50 mm and a length of 570 mm. The furnace was 510 mm long with outside diameter of 280 mm. Although chromel-alumel thermocouple was used for temperature profiling, Pt-Pt/10%Rh controller was used for actual experiments. The Pt-Pt/10%Rh controller was of (Indotherm-401) make. It was a power proportionating controller with a control sensitivity of $\pm 2^0$ C. The temperature was done with a digital millivoltmeter (AGRONIC-152) with a precision of ± 0.01 mV.

3.3.2 : Gas train

The gas train consists of cylinders of Ar, H_2, and CO_2 which were connected to different flowmeters. A schematic diagram of the gas train is shown in Fig 3.4. The flowmeters were calibrated for all the three gases with the help of wet test meter. The calibrated readings of the two flowmeters that were used for all the three gases are presented below as best fit equation and graphically in Fig 3.5 and Fig 3.6 respectively.

Flowmeter 1

$$Q_{Ar} = 0.146 + 0.13 \times \Delta h \quad (3.1)$$

$$Q_{CO_2} = -0.36 + 0.23 \times \Delta h \quad (3.2)$$

$$Q_{H_2} = -1.01 + 0.39 \times \Delta h \quad (3.3)$$

Flowmeter 2

$$Q_{Ar} = 0.18 + 0.09 \times \Delta h \quad (3.4)$$

$$Q_{CO_2} = 0.13 + 0.13 \times \Delta h \quad (3.5)$$

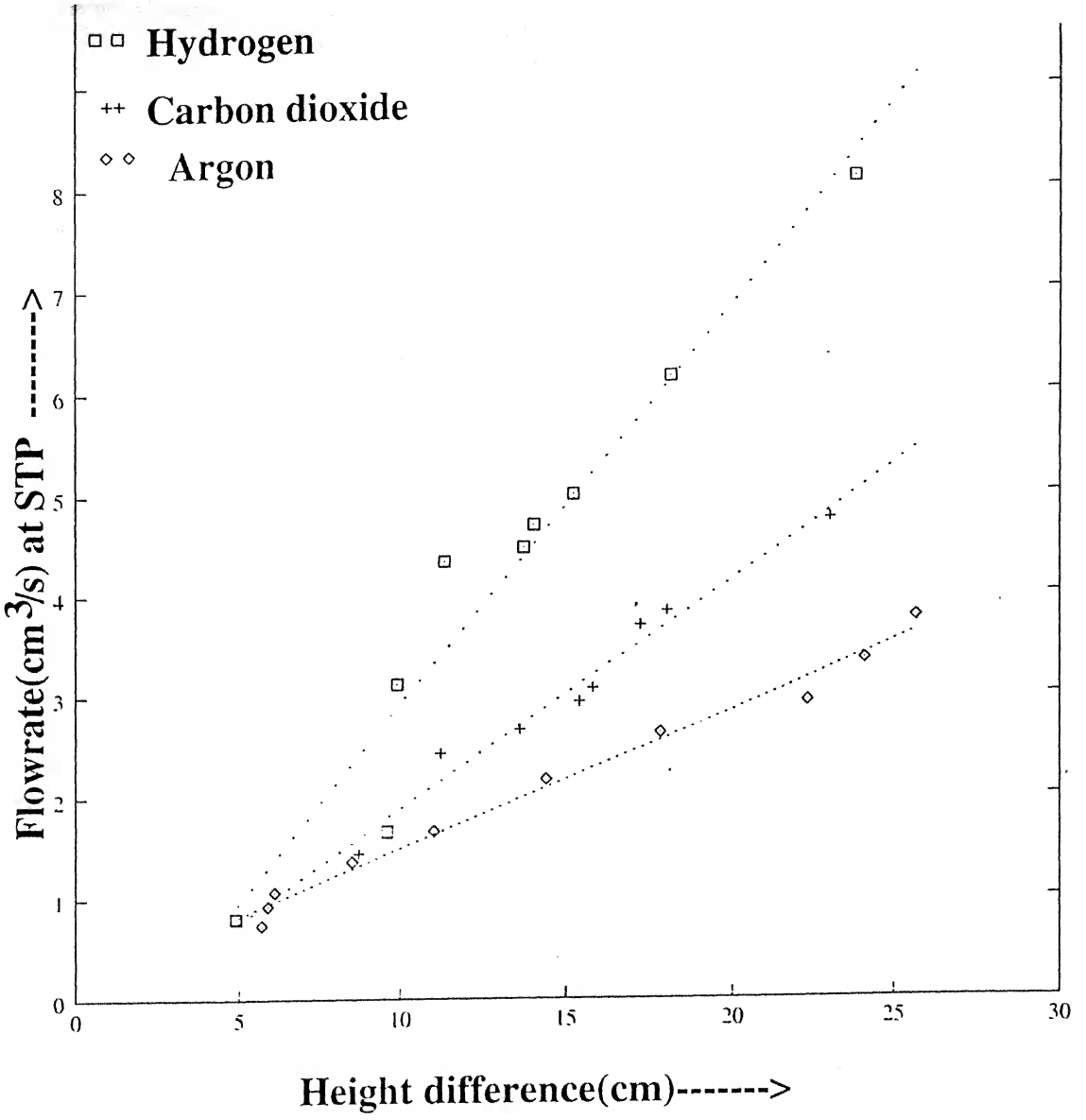

Fig.3.5: Flowmeter 1

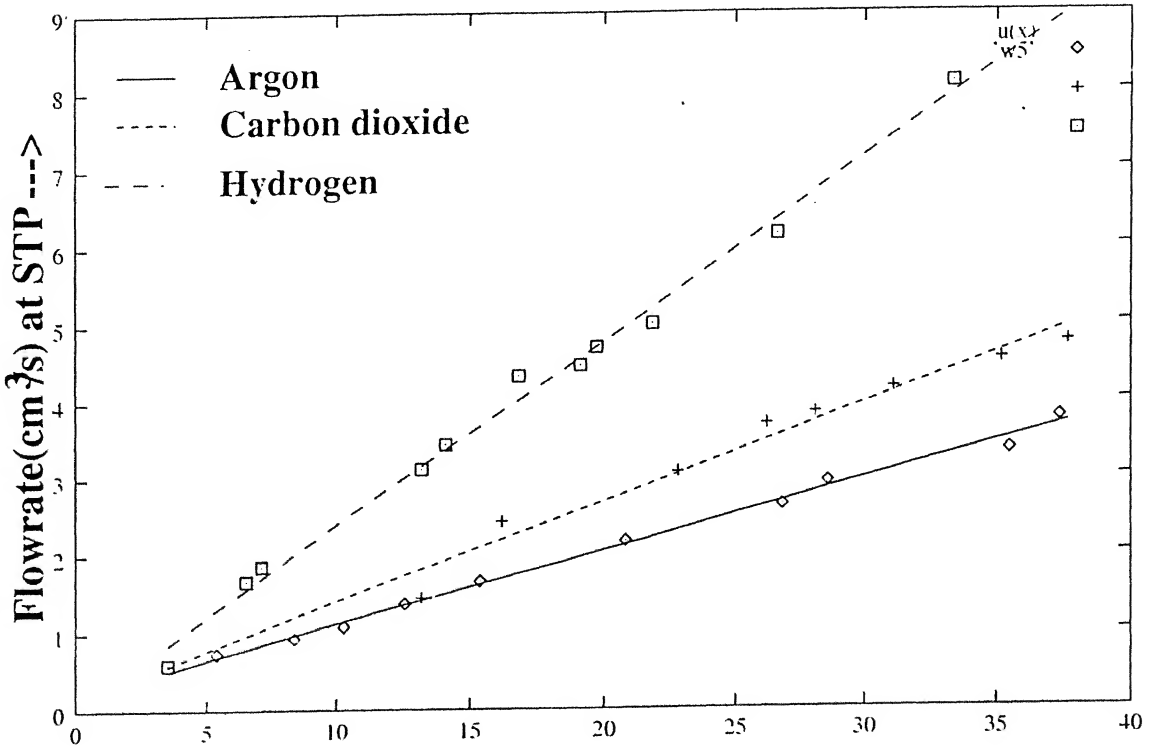

Fig.3.6:Flowmeter2

$$Q_{H_2} = 0.01 + 0.23 \times \Delta h \quad (3.6)$$

where Q = Flow rate (cm^3/s at STP) and

Δh = Height difference (Cm).

Argon was passed through a furnace containing BTS catalyst (manufactured by BASF, Germany) for removal of trace of oxygen present in it. This catalyst has fine copper particles dispersed on a porous oxide pellet. Anhydrous $CaCl_2$ tube was connection with the furnace containing the catalyst for removal of moisture. The operating temperature of the BTS catalyst furnace was 180^0 C. The BTS catalyst was regenerated time to time by treating it by hydrogen at a temperature of 180^0 C.

3.4 : Procedure for reduction experiments

3.4.1 : Reduction in Argon and mixture of CO_2 and H_2

Reduction experiments were carried out only when the furnace attained the required set temperature. Before keeping the sample in the furnace, argon was allowed to flow through the furnace chamber for nearly 5 minutes with a flow rate of approximately 5 cm^3/s. This was necessary to remove any air present in the furnace. The weighed samples were then introduced into the furnace by opening the furnace head, maintaining the flow of argon. A refractory boat containing two steel crucibles each of inner diameter of 1.1 cm and heights of 1 cm and 6 mm respectively, with mixture of iron ore fines and activated char was placed at the cold zone of the furnace for nearly one minute.

The furnace head was closed and the flow rate was adjusted to the desired value for studying reduction behaviour in argon.

In case of CO_2 and H_2 mixture, the flow rates of the two gases were adjusted as per the requirement. The boat was then slowly pushed into the hot zone of the furnace. The experiments were carried out for specified time in the desired gas. If the experiment was carried out in CO_2 and H_2 mixture, then the gas flow was stopped. The boat was taken out into the cold zone of the furnace and kept there under argon flow for 2-3 minutes. The furnace head was then removed and the boat was taken out on an asbestos sheet and covered with a cover made up of aluminium (slightly bigger in size than that of the boat) with minimum time gap so that so that there is no re-oxidation of the reduced iron. After the crucibles cooled down, they were placed in a dessicator for some time and then weighed. All weighing were done in an electronic analytical balance (Sartorius make).

3.4.2 : Procedure for determination of degree of reduction

In reduction of iron oxide with carbon, the extent of reduction cannot be found out directly from the loss in weight of the sample, since this consists of both oxygen and carbon losses. Apart from this there is a weight loss due to volatile matter and moisture if present. Since only weight loss of the sample is not sufficient, some additional measurements are required for estimating the degree of reduction (F) which is defined as follows

$$F = \frac{\text{wt. of oxygen removed from ironoxide}}{\text{total wt. of oxygen present in ironoxide}} \qquad (3.7)$$

Investigators for determination of F for composite pellets have adopted different procedures. Some chemically analysed the reduced mass, and used this information either alone or with overall weight loss in order to estimate F. Amongst them the procedure adopted by Bryk and Lu (19) was the most general, and is applicable to all types of carbonaceous reductant with or without binder.

Dutta and Ghosh (20) found earlier procedures to be unsatisfactory and carried out trials to develop a satisfactory procedure for determining F. In this procedure, further reduction of reduced composite pellets were carried out in a thermogravimetric set up in flowing hydrogen. The degree of reduction was calculated by the following equation.

$$F = \frac{W_o^i - \Delta W_o^H}{W_o^i} \qquad (3.8)$$

where W_o^i is the total weight of oxygen present in the iron oxide and ΔW_o^H is the total weight loss during hydrogen reduction.

The above procedure was examined for two possible source of error which are as follows:

(1) Loss of carbon due to reaction of residual carbon with residual oxygen in pellet during hydrogen treatment of the partially reduced pellet.

(2) loss of carbon due to reaction

$$C(s) + 2H_2(g) = CH_4(g) \qquad (3.9)$$

Considering the above factor they gave trials in order to determine how serious these sources of errors would be. After trials it was found that the error from

these sources were insignificant and pct. error may be at the most 2% at 750K for one hour at flow rate of 5 cm^3/s at STP. Dutta and others subsequently employed this procedure for determination of F and it has been adopted here.

The partially reduced mixture of iron ore activated char was crushed. The crushed sample was taken in the same crucible to which it belonged. The procedure consisted of cleaning the crucible with dil. HCl before taking fresh sample. As already stated earlier, the hot crucibles were sealed by a cover from the atmospheric air immediately upon taking out from the furnace. The crucible along with the sample was then weighed.

The furnace chamber was then flushed with argon at 5 cm^3/s for nearly 5 minutes, the furnace being at a temperature of 750^0 C. The refractory boat containing the crucibles with weighed amounts of partially reduced samples, was then inserted following the steps described for reduction experiments. The argon flow was stopped and hydrogen was passed at 3.32 cm^3/s for one hour. After one hour the sample were taken out and stored as described previously, while taking out the boat hydrogen flow was stopped and argon flow started at 5 cm^3/s. The samples were cooled as described previously. After cooling the samples were weighed and the amount of residual oxygen calculated.

Chapter 4

RESULTS AND DISCUSSIONS

4.1 : Results

All experiments were conducted with activated char as reductant. The variables were :

(1) Temperature (1150 K, 1250 K, 1300 K)

(2) Fe_2O_3/C ratio (3/1 and 4.5/1 mass ratio)

(3) Sample size (small crucible and big crucible each having inner diameter of 1.1 cm and heights of 6 mm and 1 cm respectively)

(4) 3 gas compositions (Ar, H_2:CO_2 = 1.5:1 and H_2:CO_2 = 3:1)

Therefore the experimental conditions were altogether 36 (3*2*2*3). In each condition measurements were made at five durations of the sample in the hot zone viz; 600, 1200, 1800, 2400 and 3000 secs. This makes total of 180 set of data and some of them were repeated also. Total gas flow rates were kept constant at 4 cms^{-1} (STP) for all experiments. Each experimental condition is summarized by a code, which is explained below.

1st digit is 'a', which represents the reductant used, that is activated char.

2nd and 3rd digits represent the Fe_2O_3/C ratio, that is 30 and 45 for ratios 3, 4.5 respectively.

4th and 5th digits represent the temperature, that is 11, 12, 13 for 1150, 1250 and 1300 K respectively.

6^{th} and 7^{th} digits represent the gaseous environment that is ar, H1 and H2 for argon, H_2+CO_2 mixtures with $H_2/CO_2 = 3$ and $H_2/CO_2 = 1.5$ respectively.

8^{th} digit represents the size of the pellet, that is s for small, and b for large.

For example, code a3011ars means experiment with $Fe_2O_3/C = 3$, at T = 1150 K in argon with small sample.

The following procedure was employed for calculation of degree of reduction (F).

Initial weight of the sample = W_s

Sample contains blue dust and activated char

Weight of blue dust in the sample (W_{bd}) =

$$\left[\frac{\text{Wt. of blue dust}}{\text{Wt. of (bluedust + activated char)}}\right]_{\text{in mixture}} \times W_s \qquad (4.1)$$

Amount of Fe_2O_3 in the sample = W_{bd} * 0.954 (4.2)

Initial weight of oxygen in the sample associated with Fe_2O_3 =

$$WiO = W_{bd} * 0.954*0.3 \qquad (4.3)$$

Since Fe_2O_3 contains 0.3 fraction oxygen.

$$F = \frac{WiO - \Delta W_o^H}{WiO} \qquad (4.4)$$

W_o^H is the total weight loss during hydrogen reduction. Appendix A 1.1, A 1.2, A 1.3 present data. F versus t data for each experimental condition was fitted with a polynomial of the following form

$$F = a + bt + ct^2 + dt^3 + et^4 \qquad (4.5)$$

Where a, b, c, d, e are empirical coefficients and t is in sec. The co-efficients were evaluated by regression analysis using standard GNUPLOT. The values of the coefficients have been reported in Appendix A 1.1, A 1.2, A 1.3.

4.2 : Discussions of Results

4.2.1 : General Features for Reaction under argon

In argon the exit gas would consist of Ar + CO + CO_2, the latter resulting from the reaction of Fe_2O_3 with carbon. The argon is simply an inert flushing gas. Here the reaction mechanism and kinetics are relatively simple.

Chapter 1 has briefly summarised the mechanism and kinetics of the reduction of iron oxide by carbon under inert atmosphere. To summarise, the reaction is dominently controlled by rate of gasification of carbon by CO_2. Again it is largely chemically controlled as deduced from observations such as

(a) high activation energy

(b) strong retarding influence of product gas (carbon monoxide) on the rate

(c) catalytic enhancement of rate by reduced metallic iron.

4.2.2 : Thermodynamic considerations for H_2-CO_2 gas mixture

When a mixture of H_2 and CO_2 is introduced into a higher temperature zone, it undergoes water gas shift reaction

$$H_2(g) + CO_2(g) = H_2O(g) + CO(g) \qquad (4.6)$$

The equilibrium constant for this is given by

$$K = \left[\frac{p_{H_2O} \times p_{CO}}{p_{H_2} \times p_{CO_2}} \right]_{eq} \quad (4.7)$$

Again $p_{H_2} + p_{H_2O} + p_{CO} + p_{CO_2} = 1\,atm$ (4.8)

For a given p_{H_2}/p_{CO_2} ratio at the inlet, therefore equilibrium p_{CO}/p_{CO_2} ratio can be calculated from the above equations if K is known.

Again $\Delta G^0 = -RT \ln K$ (4.9)

ΔG^0 for reaction (4.6) can be calculated from data on ΔG^0 of formation of H_2O, CO_2 and CO as follows,

$$\Delta G^0 = \Delta G_f^0(CO) + \Delta G_f^0(H_2O) - \Delta G_f^0(CO_2) \quad (4.10)$$

where ΔG_f^0 means standard free energy of formation of a compound. Based on the standard ΔG_f^0 values from standard thermodynamic source[21], values of K and also the values of gas compositions at 1150, 1250 and 1300 K and p_{H_2}/p_{CO_2} ratios of 3 and 1.5 are presented in Table 4.1.

It's fairly easy, thermodynamically speaking, to reduce Fe_2O_3 into Fe_3O_4, and Fe_3O_4 into FeO. However it requires a high concentration of CO in CO/CO_2 mixture to reduce Fe_xO into Fe. This is illustrated in Fig 4.0.

Hence it is important to calculate p_{CO}/p_{CO_2} equilibrium value for the reaction:

$$Fe_xO(s) + CO(g) = xFe(s) + CO_2(g) \quad (4.11)$$

Table 4.1

Temperature	Equilibrium (pco/pco$_2$) for Fe_xO + Fe	For water gas shift reaction		
		K	Gas ratio	Equilibrium (p_{CO}/p_{CO_2})
1150	1.706	1.18	$H_2:CO_2 = 3:1$	3.4
			$H_2:CO_2 = 1.5:1$	1.66
1250	2.06	1.44	$H_2:CO_2 = 3:1$	4.2
			$H_2:CO_2 = 1.5:1$	1.96
1300	2.234	1.76	$H_2:CO_2 = 3:1$	4.65
			$H_2:CO_2 = 1.5:1$	2.12

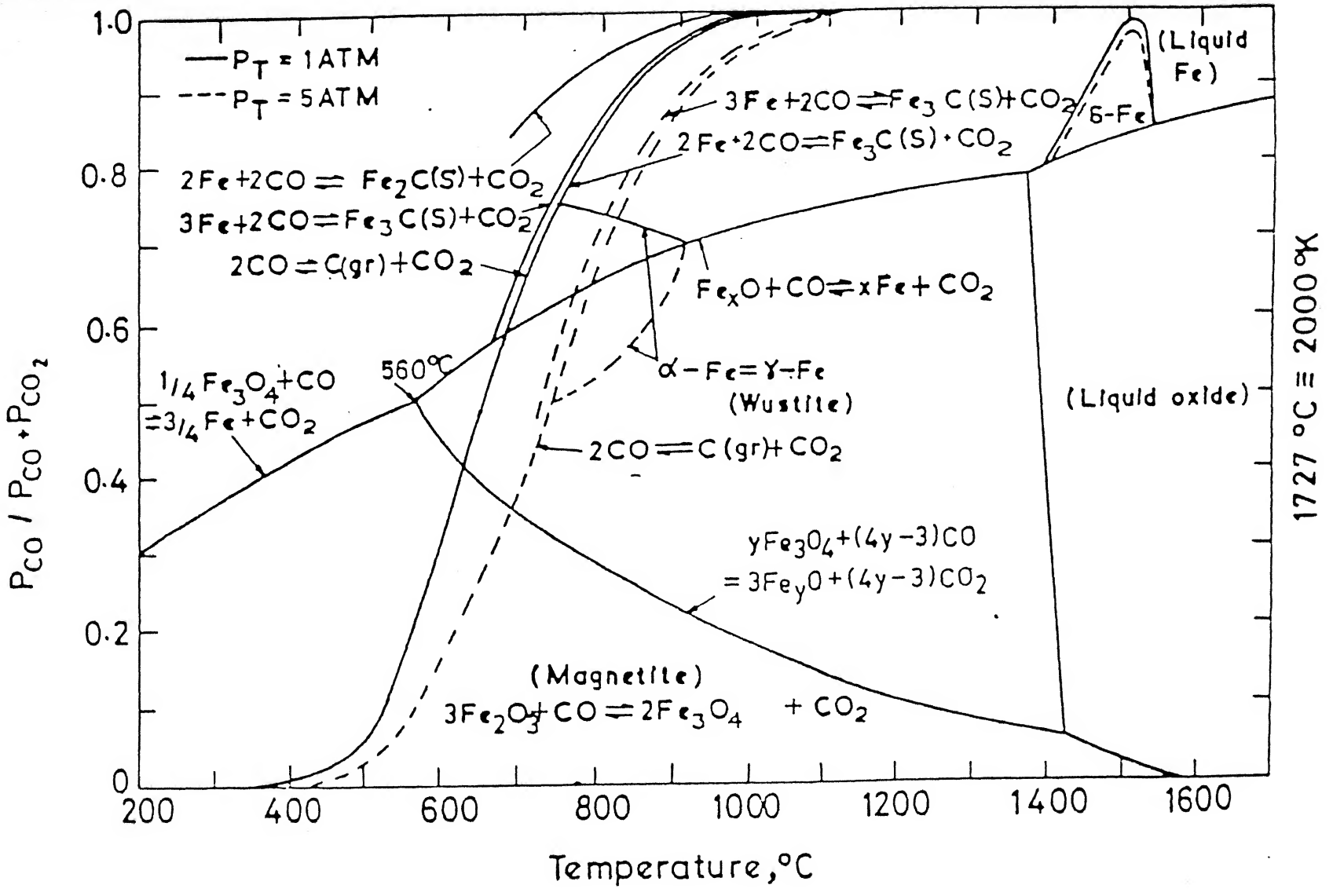

Fig 4.0 : Equilibrium diagram for Fe-C-O system

Based on the free energy data from the same source these were calculated and are presented in Table 4.1.

It may be noted from Table 4.1 that, assuming attainment of equilibrium of water gas shift reaction in furnace hot zone, the gas mixture with H_2/CO_2 ratio of 3 is reducing to wustite. On the other hand the gas mixture with H_2/CO_2 with 1.5 is not reducing to wustite. Actually the experimental conditions were designed to be this way and that is why these two ratios were picked up.

As noted in chapter 3 that some earlier investigations have established that the water gas shift reaction attains equilibrium very fast at these temperatures. In order to allow this attainment of equilibrium, the total gas flow rate was kept at a moderate value of 4 $cm^3\ s^{-1}$ based on observation by Darken and Gurry[22].

4.2.3 : General Kinetic considerations for Reduction Behaviour in Gas Mixtures

In view of the water gas shift reaction, the gas at high temperature would consist of CO_2, H_2O, CO and H_2, when a mixture of H_2 + CO_2 is introduced. For understanding reduction behaviour of the oxide, therefore, the following additional considerations have to be kept in mind in addition to those which were discussed in Sec 4.2.1 for experiments under argon reduction.

(1) Two additional gaseous species, viz, H_2 and H_2O are present. H_2 is expected to reduce iron oxide. Also both H_2 and H_2O influence the rate of gasification of carbon significantly. Actually H_2O oxidizes carbon like CO_2.

(2) The concentration of CO and CO_2 in the gas will be dictated considerably by the water gas shift reaction, and this in turn will have their influence on both on the gasification reaction as well as reduction reaction.

4.2.4 : Variation of degree of reduction(F) with time

Figures 4.1 to 4.12 show variations of F with time. As stated in Sec 4.1, there are 36 experimental conditions. Each figure has data for 3 gaseous atmosphere at fixed conditions otherwise. Hence 12 figures were required. These have been arranged this way in order to visualise influence of gaseous atmosphere on reduction behaviour. The curves in the figure represent the equations based on polynomial regression fitting of the empirical equation (4.5). Original experimental data points also have been included.

In order to discuss these results in more clear and concise fashion, Table 4.2 has been prepared as guide. Table 4.2 summarizes the conditions as well as general observations on each figure. From these the following points may be noted.

(1) The degree of reduction is highest for almost all conditions for inlet gas mixture of H_2/CO_2 ratio of 3 in comparision to other two gaseous environments. This is expected since, as per the thermodynamic calculations presented in Table 4.1, this gas mixture generates an atmosphere which is reducing to Fe_xO. The flowing gas is therefore expected to participate in reduction of iron oxides since H_2

is five to ten times faster reductant as compared to CO this will contribute to enhancement of reduction further.

(2) By and large in most cases, the degree of reduction is lowest with inlet gas of H_2/CO_2 ratio equal to 1.5. As Table 4.1 shows that this gas mixture generates a p_{CO}/p_{CO_2} ratio, according to thermodynamic calculations, which is somewhat lower than that for the equilibrium of $Fe_xO \rightarrow Fe$ system. Therefore this will have a tendency to prevent reduction of Fe_xO into Fe. Stoichiometrically, two of every three atoms of Fe_2O_3 are removed in the $FeO \rightarrow Fe$ stage as follows :

$3Fe_2O_3 \rightarrow 2Fe_3O_4 \rightarrow 6FeO \rightarrow 6Fe$. That means out of every nine oxygen atoms in association with Fe_2O_3, six atoms get removed during $FeO \rightarrow Fe$ stage. Hence if $FeO \rightarrow Fe$ reduction is prevented degree of reduction should not exceed approximately 0.33. However it is larger than that in all cases, due to simultaneous reduction by activated char.

However there are some experimental conditions where the above generalisations do not hold good. Since the mechanism and kinetics of the reaction are complex, as stated in sec 4.2.3, only brief remarks would be made on these as follows.

(1) At 1150 K the behaviour pattern noted in Table 4.2 is as expected with reference to the discussions above.

(2) At 1250 K and 1300 K the degrees of reduction in argon even at 600 sec are fairly high. Moreover they do not show too much of an increase with time. The activation energy for reduction by carbon is

Table 4.2 : Observations on F versus t behaviours

T (K)	Sample Size	Fe_2O_3 C Ratio	Fig no.	Observations (Relative magnitude of F)		
				$H_2/CO_2 = 3:1$	$H_2:CO_2 = 1.5:1$	Ar
1150	Big	3	4.1	Highest	Lowest	Middle
	Big	4.5	4.2	Highest	Lowest	Middle
	Small	3	4.3	Highest	Lowest	Middle
	Small	4.5	4.4	Highest	Lowest	Middle
1250	Big	3	4.5	Lower than Ar in beginning,highest towards end	Lowest	Highest in beginning, middle towards end
	Big	4.5	4.6	In middle in the beginning, highest at the end	Lowest	Highest in beginning, middle towards end
	Small	3	4.7	Highest	Lowest	Middle
	Small	4.5	4.8	Middle in the beginning highest at the end	Lowest in the beginning, middle at the end	Highest in beginning, lowest at the end
1300	Big	3	4.9	Highest in the beginning, middle at the end	Lowest in the beginning, Highest at the end	Lowest
	Big	4.5	4.10	Highest	Lowest in the beginning, middle at the end	Highest in the beginning, Lowest at the end
	Small	3	4.11	Highest	Middle	Lowest
	Small	4.5	4.12	Highest	Comparable with Ar till t=1800 sec, middle at end	Comparable with $H_2:CO_2=1.5:1$ till t=1800 sec, Lowest at the end

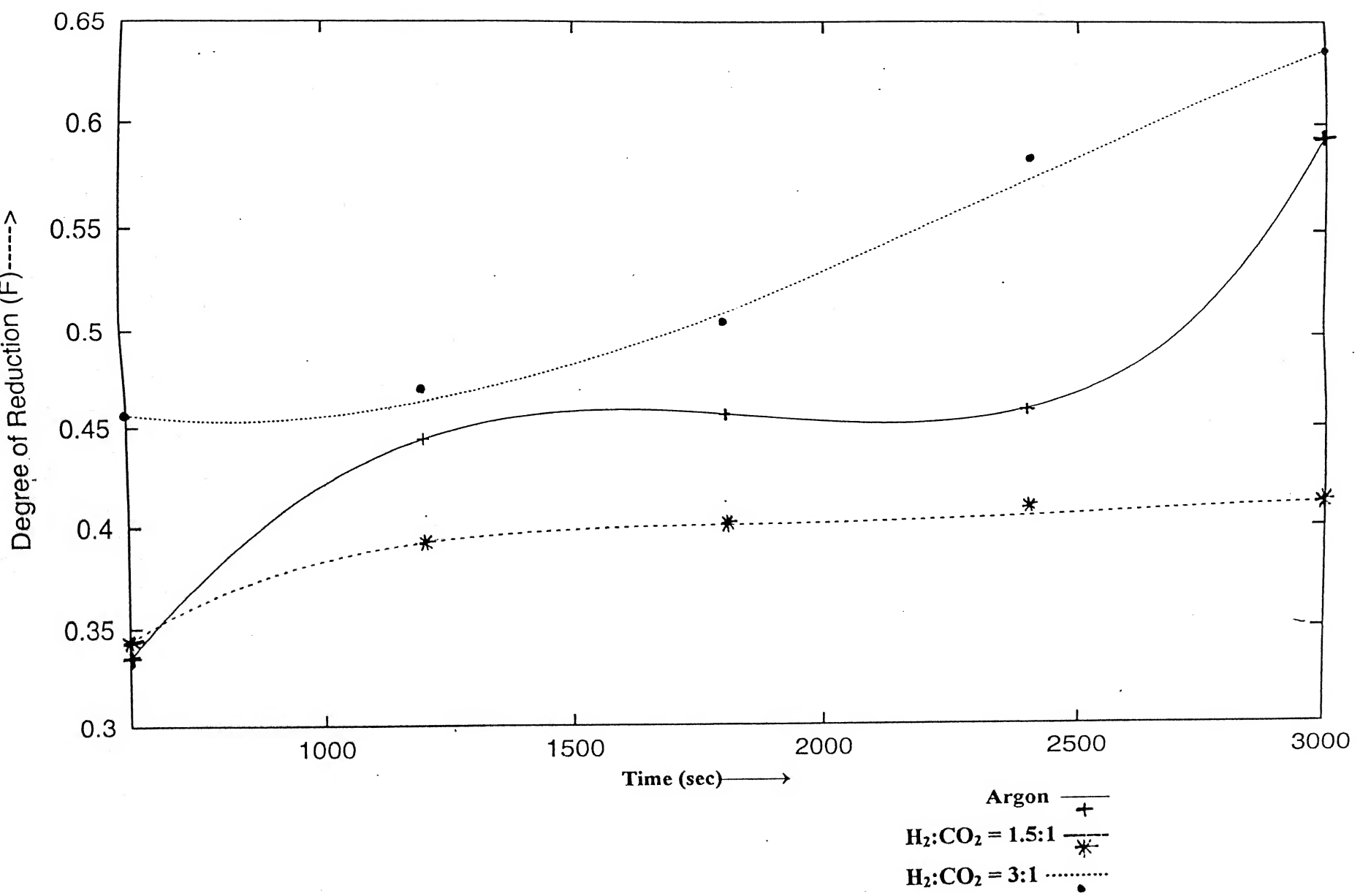

Fig 4.1 : Variation of F with time for $Fe_2O_3/C = 3$, big sample size at 1150K

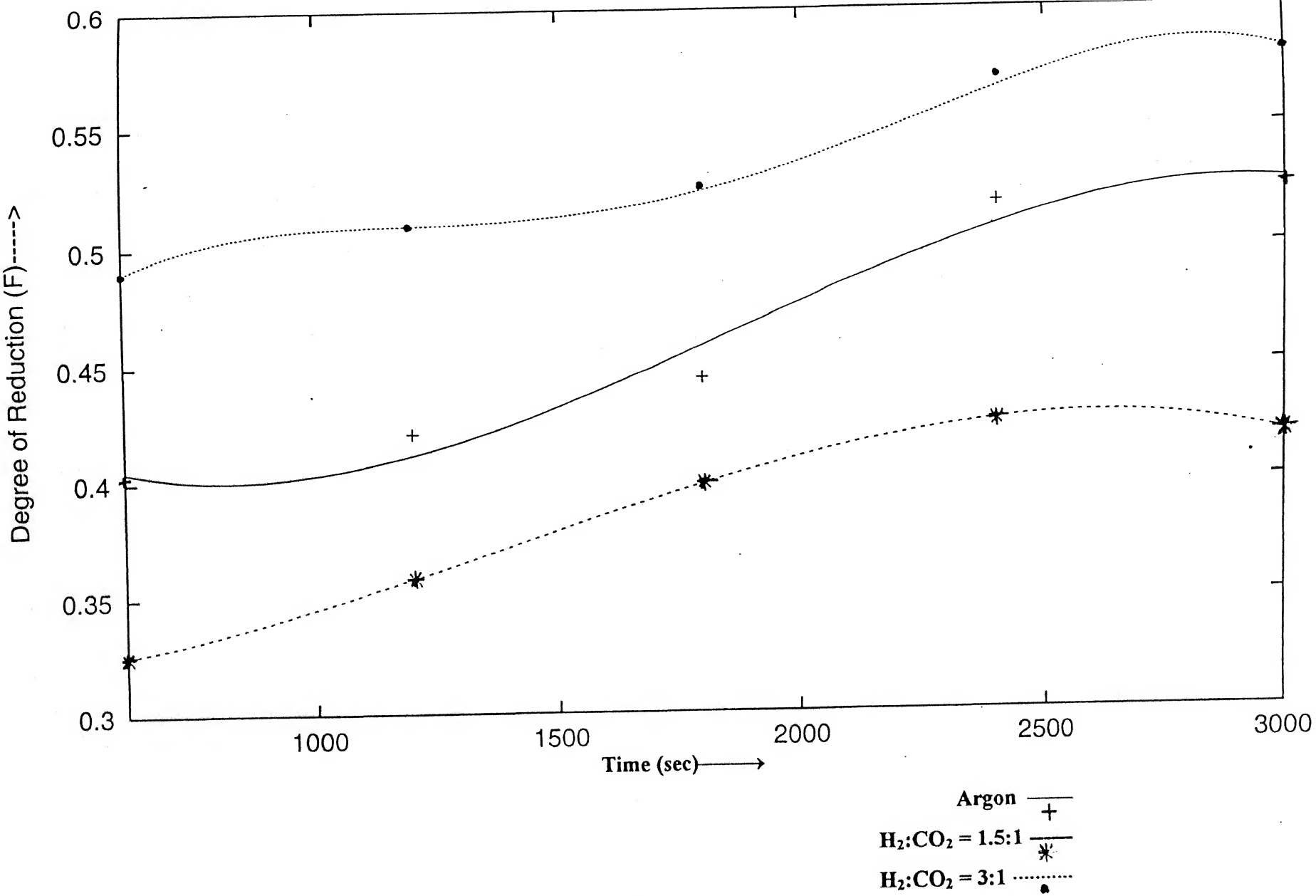

Fig 4.2 : Variation of F with time for $Fe_2O_3/C = 4.5$, big sample size at 1150K

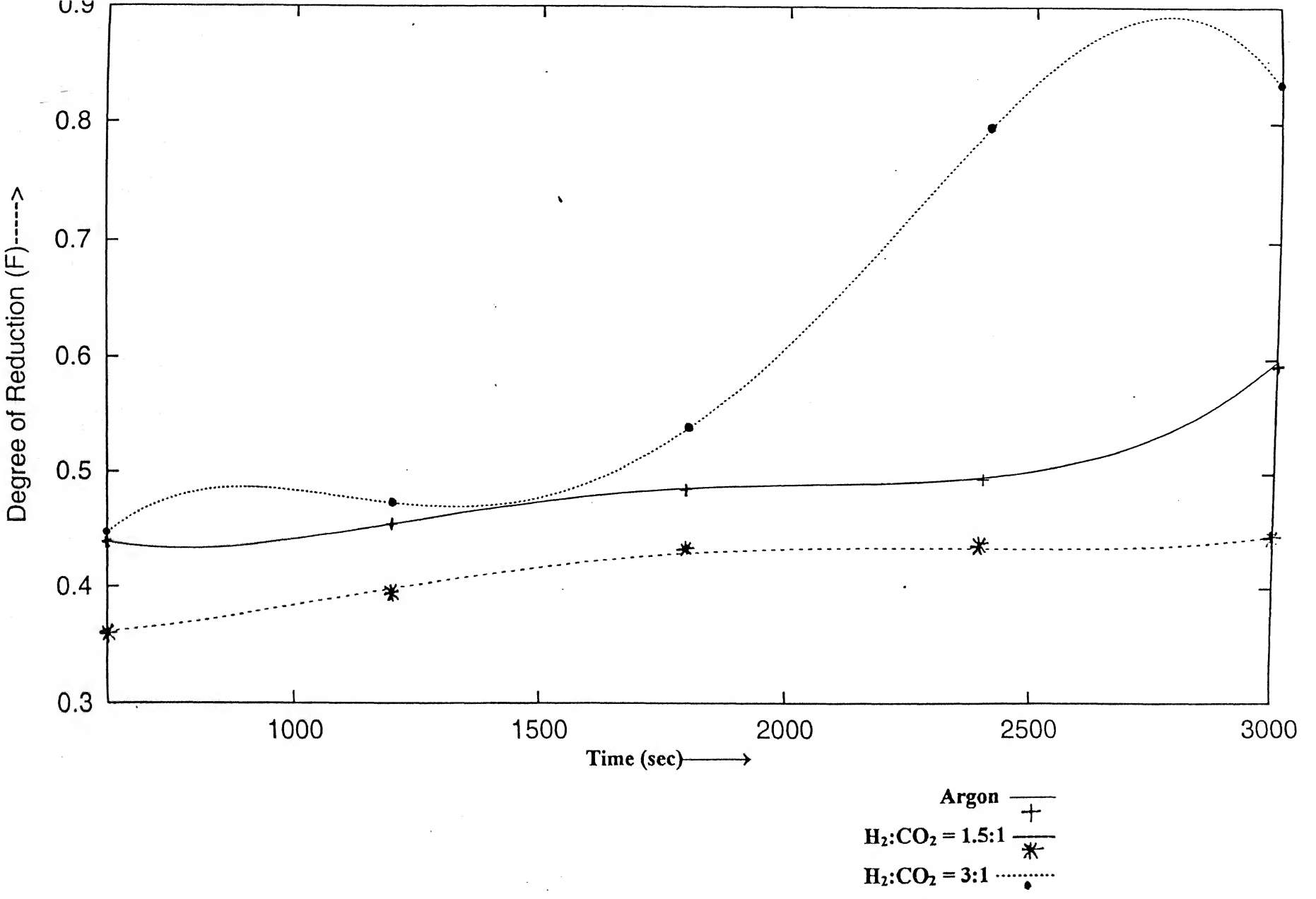

Fig 4.3 : Variation of F with time for $Fe_2O_3/C = 3$, small sample size at 1150K

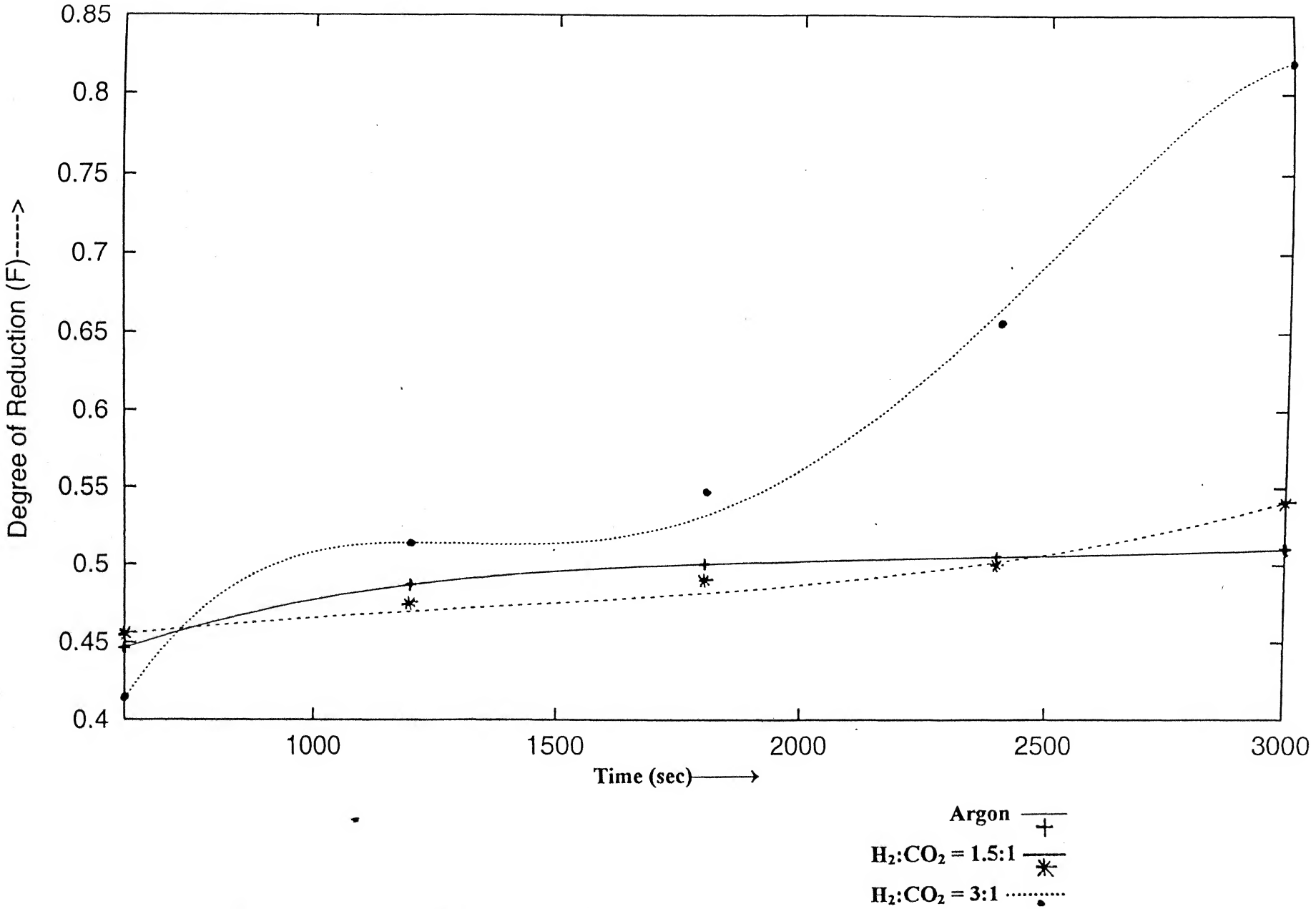

Fig 4.4 : Variation of F with time for Fe_2O_3/C = 4.5, small sample size at 1150K

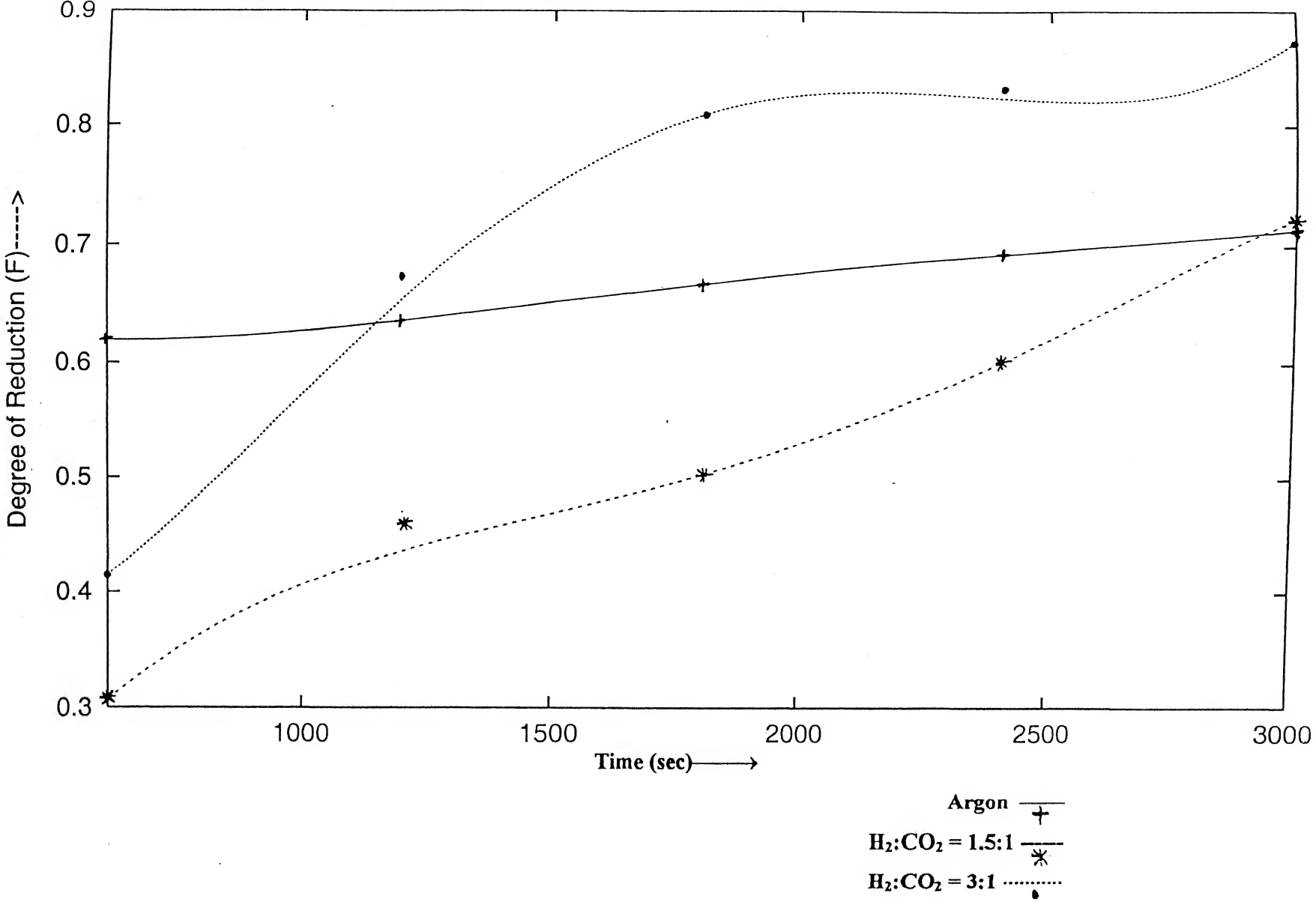

Fig 4.5 : Variation of F with time for $Fe_2O_3/C = 3$, big sample size at 1250K

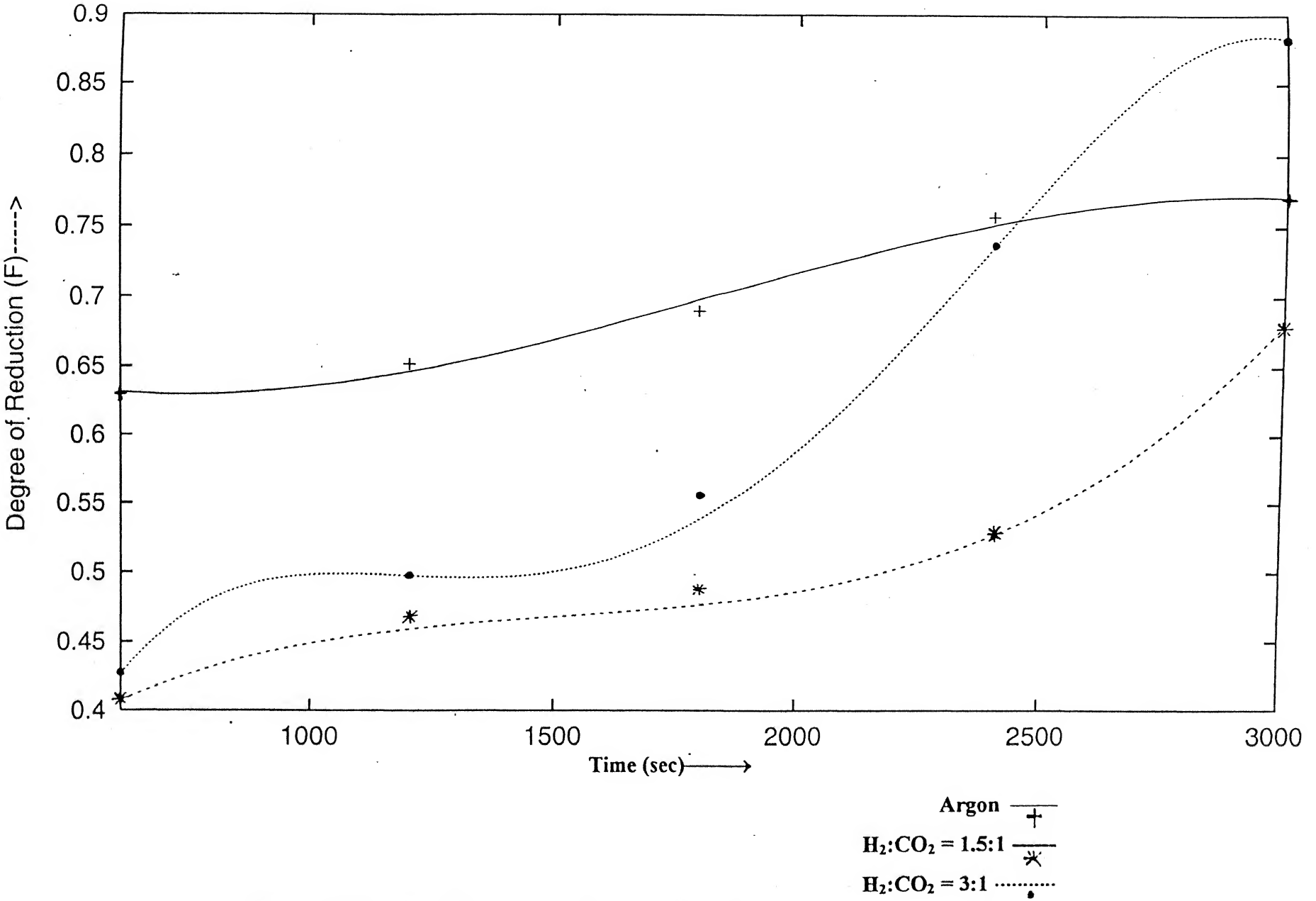

Fig 4.6 : Variation of F with time for $Fe_2O_3/C = 4.5$, big sample size at 1250K

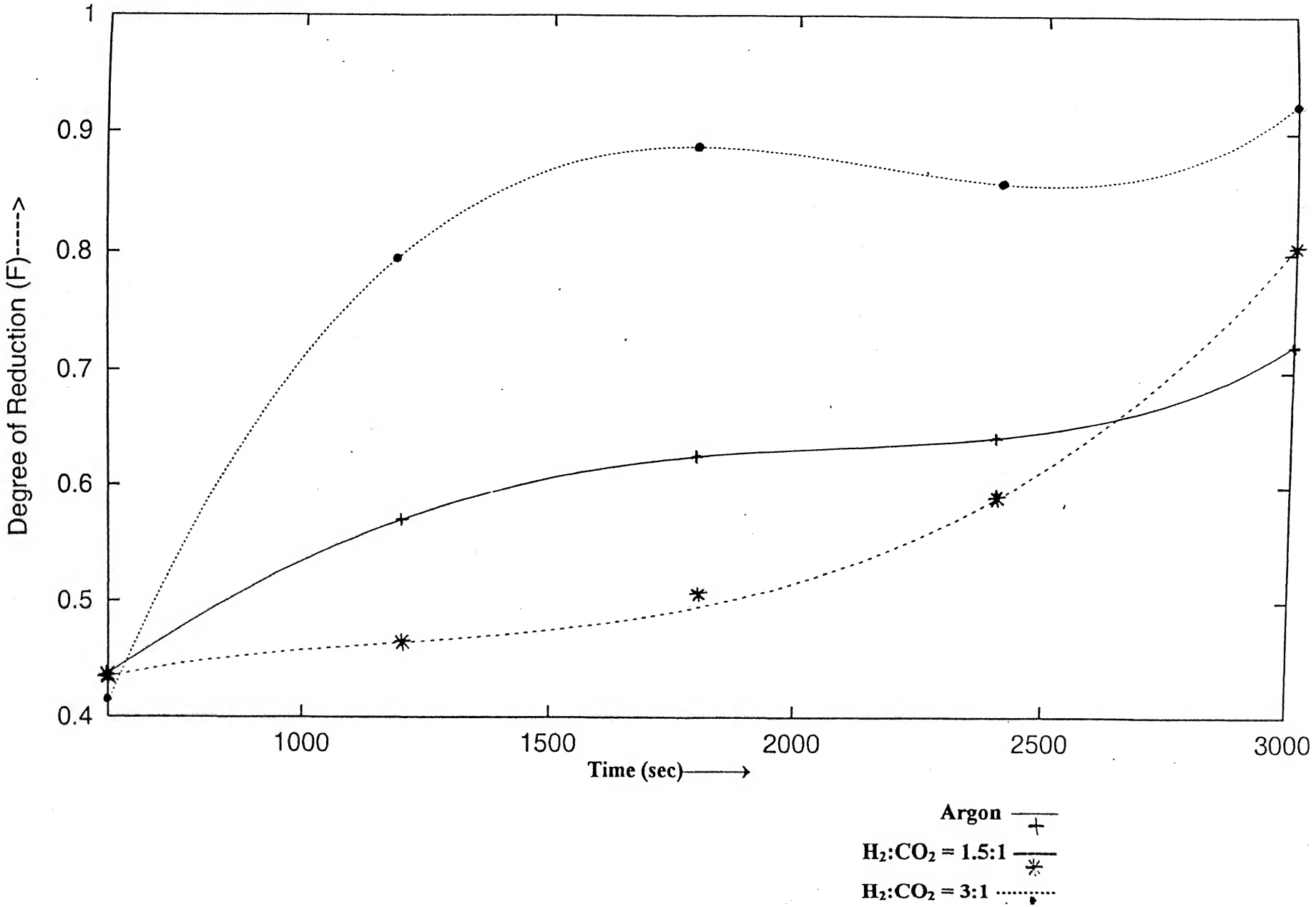

Fig 4.7 : Variation of F with time for $Fe_2O_3/C = 3$, small sample size at 1250K

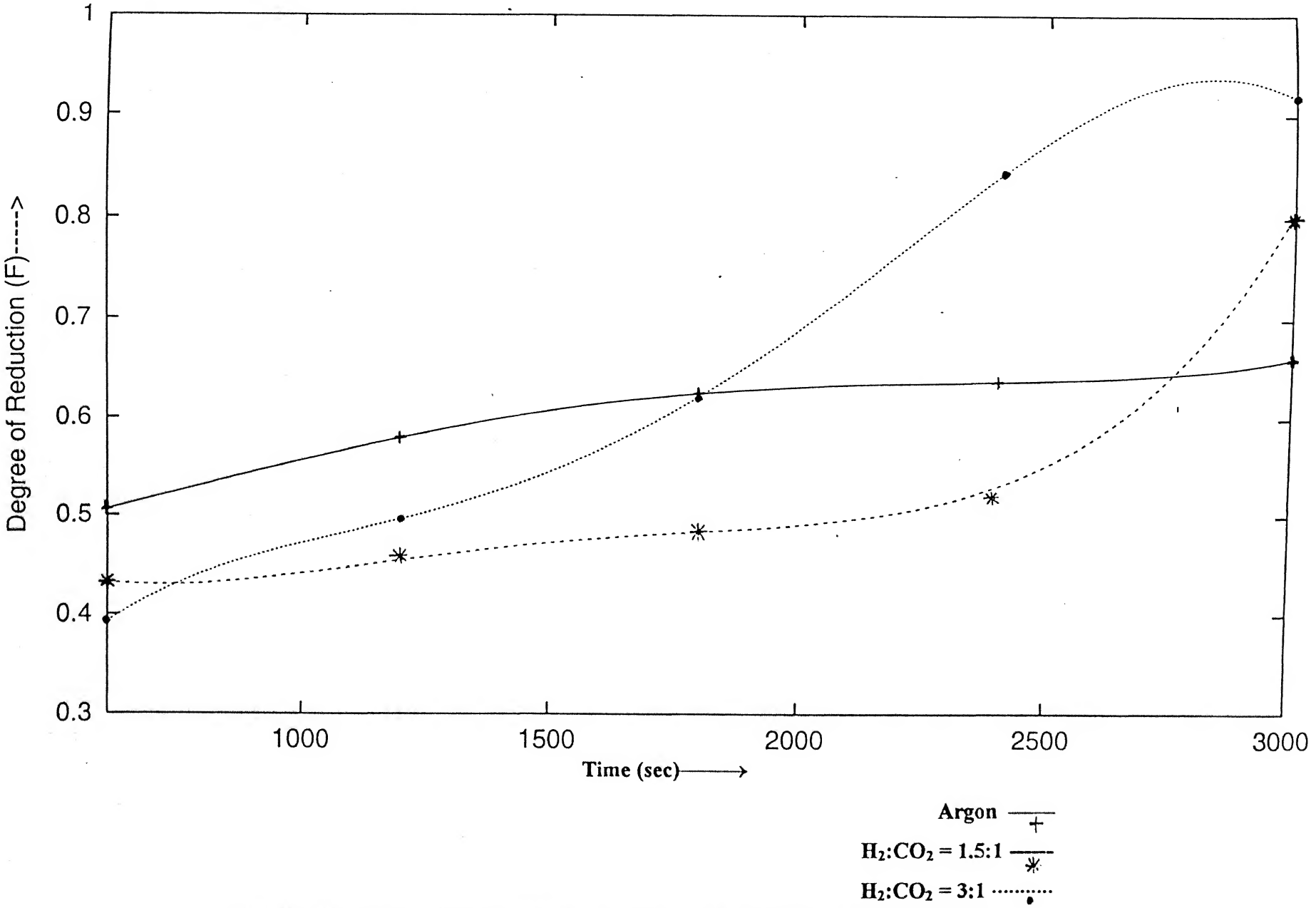

Fig 4.8 : Variation of F with time for $Fe_2O_3/C = 4.5$, small sample size at 1250K

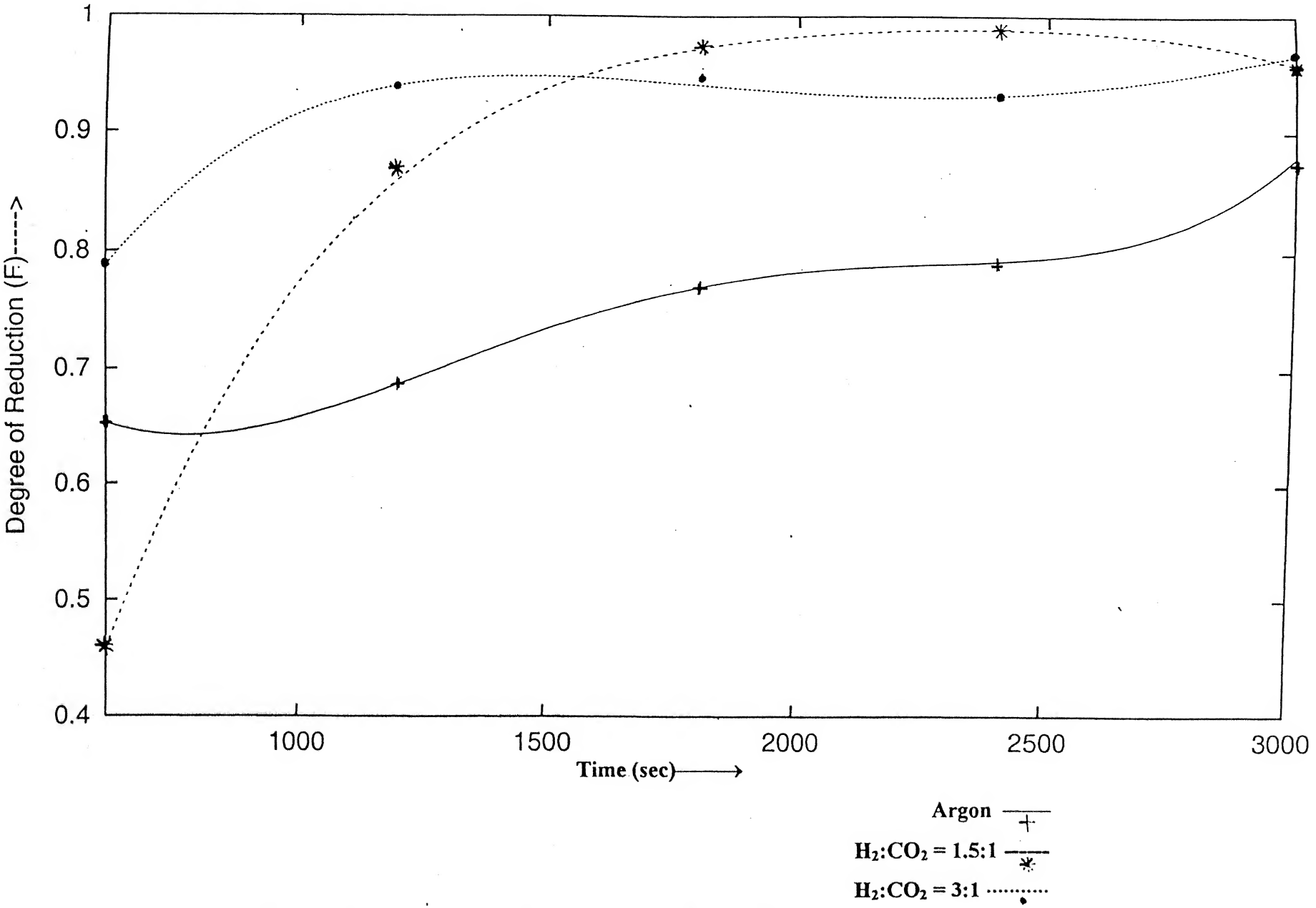

Fig 4.9 : Variation of F with time for $Fe_2O_3/C = 3$, big sample size at 1300K

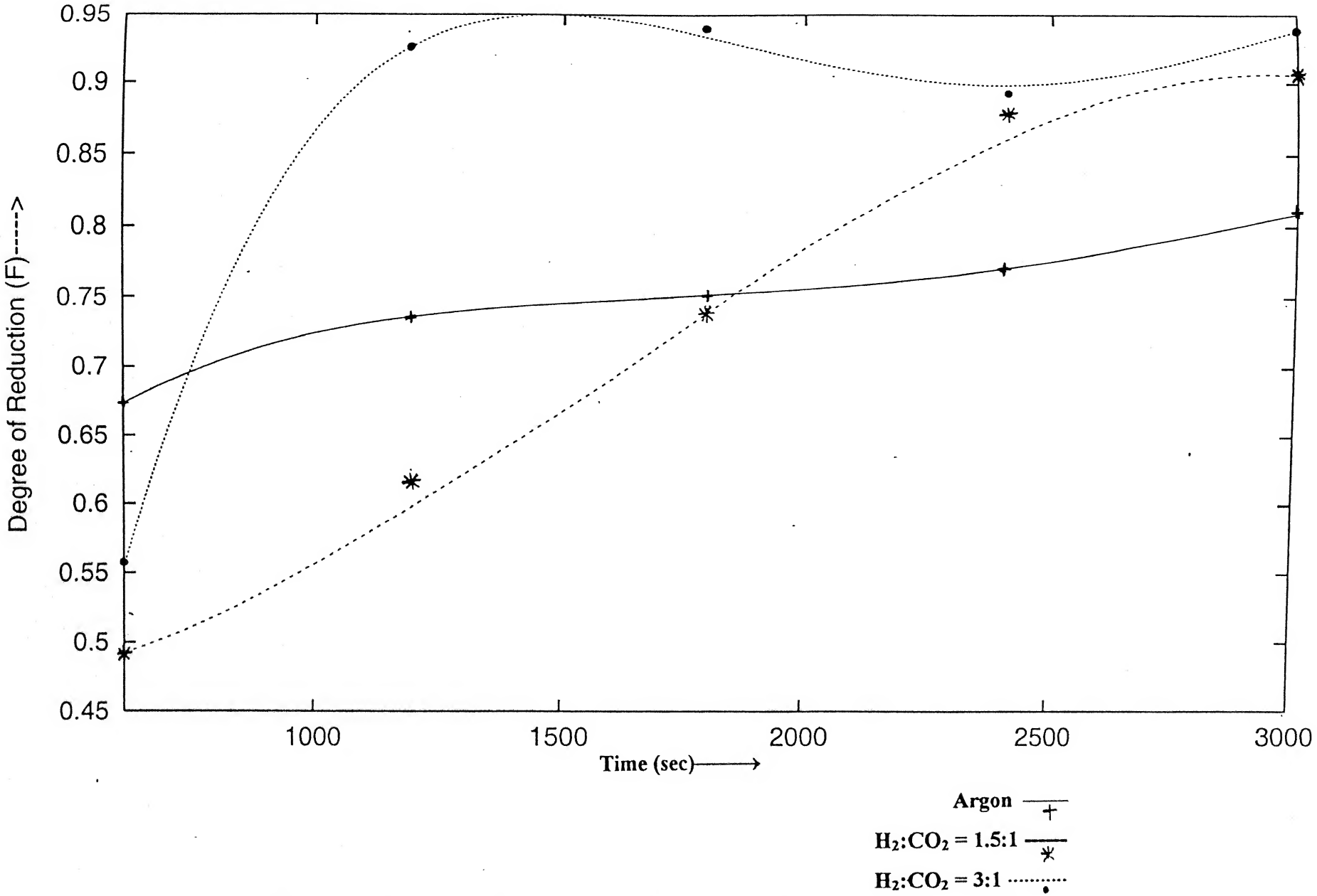

Fig 4.10 : Variation of F with time for Fe_2O_3/C = 4.5, big sample size at 1300K

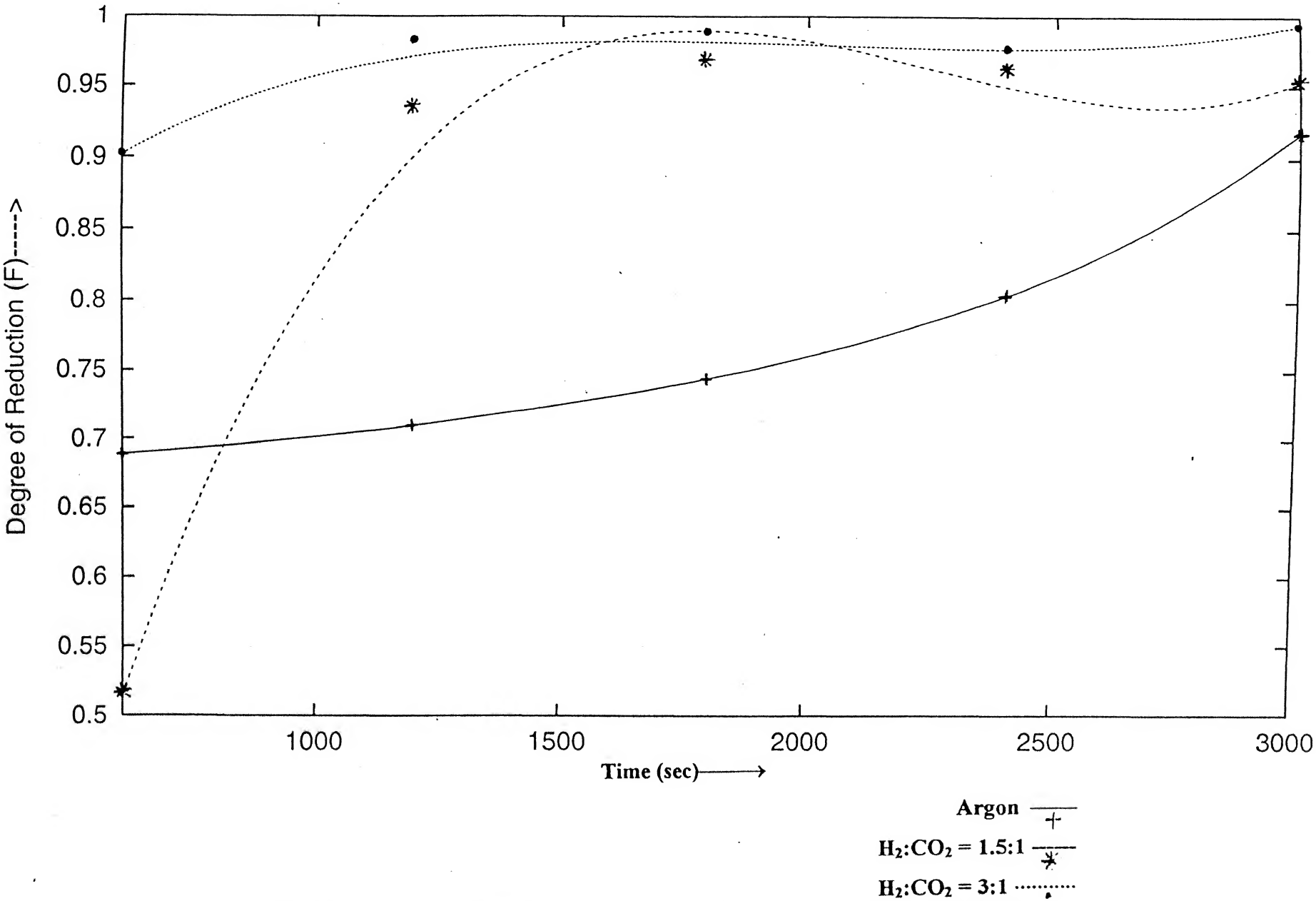

Fig 4.11 : Variation of F with time for $Fe_2O_3/C = 3$, small sample size at 1300K

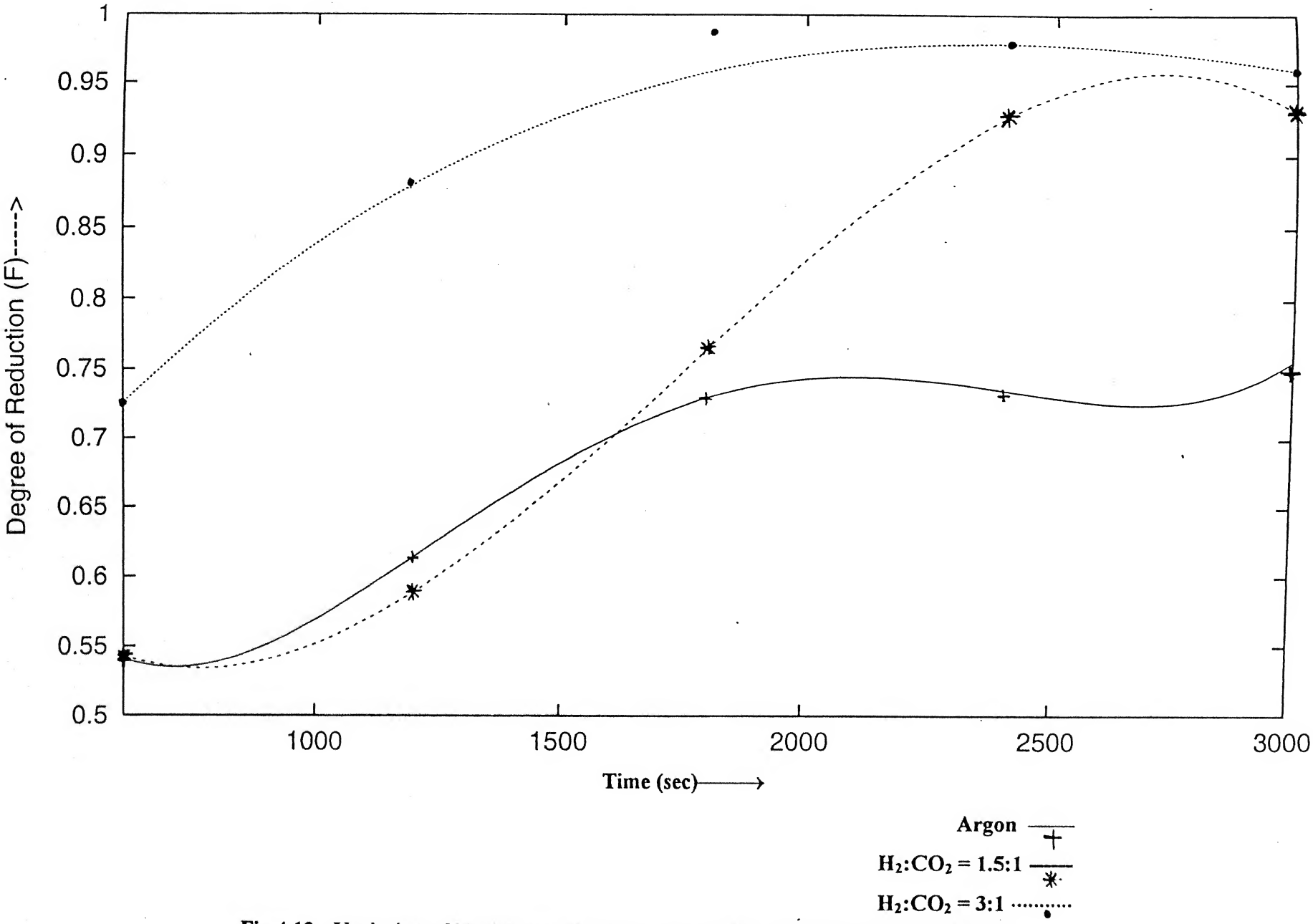

Fig 4.12 : Variation of F with time for $Fe_2O_3/C = 4.5$, small sample size at 1300K

much larger (240-300 $KJmol^{-1}$) as compared to those of gaseous reduction (40-100 $KJmol^{-1}$). Therefore the reduction by carbon will be more dominating as compared to the gaseous reduction. However it is not clear as to why F did not increase substantially with time. As stated earlier the samples with Fe_2O_3/C equal to 4.5, stoichiometrically speaking had sufficient carbon to reduce all Fe_2O_3. Samples with Fe_2O_3/C equal to 3 had stoichiometrically excess carbon.

(3) The above comments grossly explain the behaviour pattern in Fig 4.5 and 4.6 at 1250 K. In Fig 4.6 Fe_2O_3/C ratio was 4.5 and in Fig 4.5 the ratio was 3. From this point of view the reduction under argon should have been more dominating in Fig 4.5 than in Fig 4.6. However the actual situation is reverse.

(4) At 1300 K for all samples, there has been considerably larger reduction in H_2/CO_2 ratio of 1.5. Only possible explanation again is enhancement of rate of gasification reaction and its consequence effect on reduction behaviour.

4.2.5 : Variation of degree of reduction with temperature

As Fig 4.1 to 4.12 reveal, the effect of temperature on degree of reduction is not going to be the same at different times. In order to visualise influence of temperature therefore, it was decided to plot F at 2000 sec as function of temperature. Fig 4.13 presents this for various experimental conditions. The curves in Fig 4.13 are based on the polynomial fitted equations. The reason for choosing time equal to 2000 sec is to avoid both initial and final times because

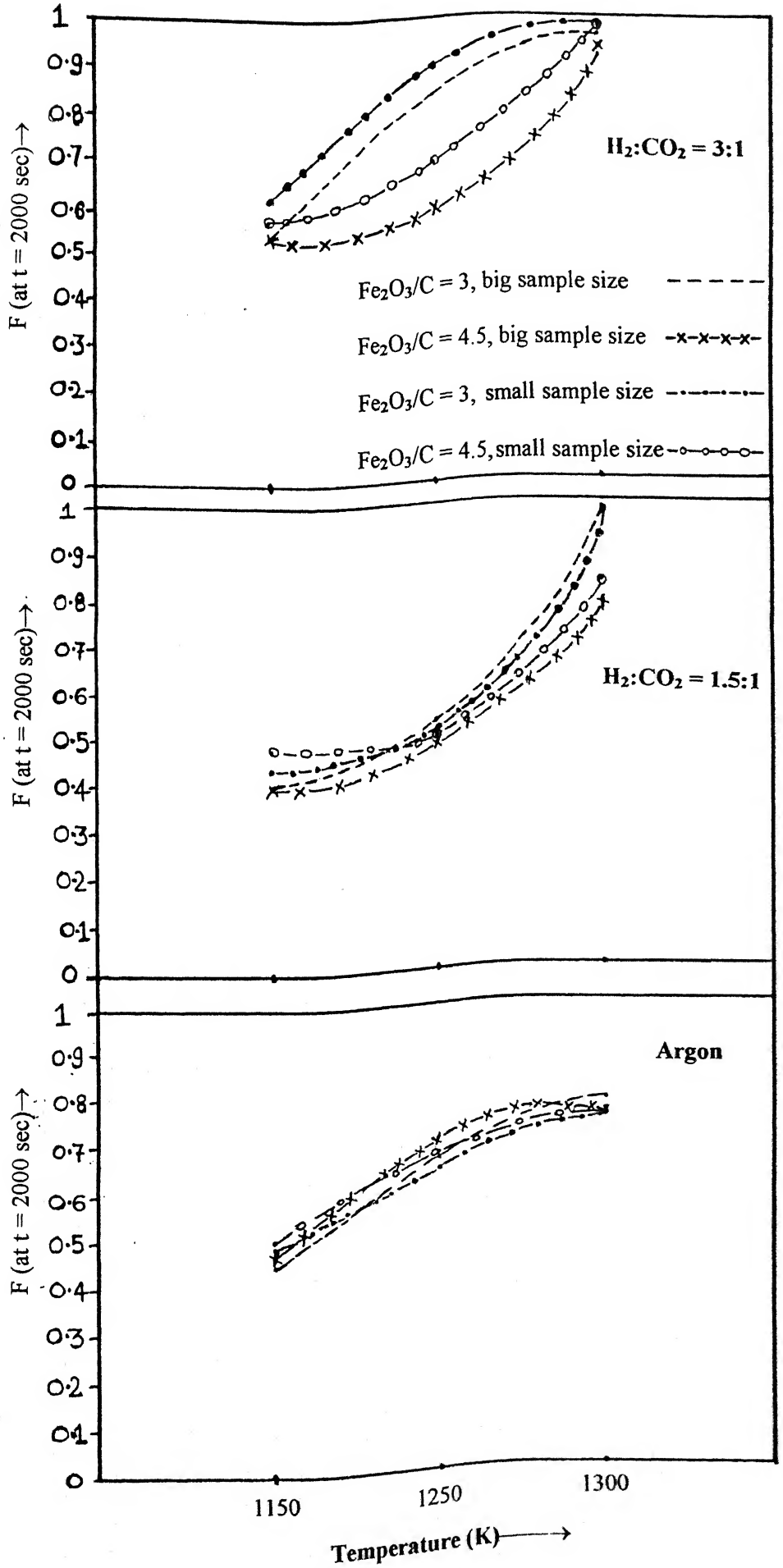
F (at t = 2000 sec)→
1
0·9
0·8
0·7
0·6
0·5
0·4
0·3
0·2
0·1
0
H₂:CO₂ = 3:1
Fe₂O₃/C = 3, big sample size
Fe₂O₃/C = 4.5, big sample size
Fe₂O₃/C = 3, small sample size
Fe₂O₃/C = 4.5, small sample size
H₂:CO₂ = 1.5:1
Argon
1150
1250
1300
Temperature (K)→

(1) Initially the conditions are more complicated because the reactions are endothermic and it has been established in literature that it takes 400-600 sec approximately to attain steady state temperature and condition in the sample.

(2) At 3000 sec the quantity of carbon as well as Fe_2O_3 remaining in the sample will be small fractions. This is not representative of the sample. Hence 2000 sec was chosen as the time.

Examination of Fig 4.13 reveals the following behaviour patterns.

(1) For all conditions F increases with Temperature

(2) For H_2/CO_2 ratio of 3, the comparision of the four curves are as per expectations i.e, bigger samples showing lower values of F, also samples with Fe_2O_3/C equal to 3 showing higher rates as compared to those having Fe_2O_3/C equal to 4.5, since the former has excess carbon.

(3) In argon, F at 1300 K are less than 0.8.

(4) In contrast the value of F are almost 1 (i.e, almost complete reduction of oxide) in 2000 sec in both H_2+CO_2 gas mixtures.

As discussed earlier a high degree of reduction in H_2/CO_2 ratio 3 is expected. However an interesting finding is that values of F at 1300 K in H_2/CO_2 equal to 1.5 and for Fe_2O_3/C equal to 3, were almost 1. Also for increase in temperature from 1250 to 1300 K, large increase of F may be noted for this gas composition. As discussed earlier that the gas as such is expected to be oxidising to FeO. Hence the only explanation for such high reduction is

significantly high rate of gasification in this gas mixture and consequent increase of degree of reduction.

This observation is of relevance to reduction of composite pellets in industrial gaseous atmospheres containing H_2, H_2O, CO and CO_2. Thus even if the gas mixture is thermodynamically oxidising to FeO, there is a likelyhood of achieving very high degree of reduction if the temperature is high enough and the sample has some excess carbon.

4.2.6 : Discussions on rates of reduction

A measure of rate of reduction is dF/dt. It is obtained by differentiating the eq (4.5) and is represented by

$$\frac{dF}{dt} = b + 2ct + 3dt^2 + 4et^3 \qquad (4.6)$$

In view of complex mechanism and kinetics as well a range of behaviour patterns of F versus t curves (Fig 4.1 to Fig 4.12) it is difficult to scientifically explain variation of dF/dt with time. Hence only a few dF/dt versus time curves are being presented to show the various behaviour patterns. No explains would be attempted.

Variation of dF/dt with temperature may be represented by an Arrhenius type of equation, i.e,

$$\frac{dF}{dt} = Ae^{-Q/RT} \qquad (4.12)$$

$$\log\frac{dF}{dt} = \log A - \frac{Q}{2.303 \times R \times T} \qquad (4.13)$$

Table 4.3 : log(dF/dt) and Temperature Coefficient (Q) for t = 600 and 2100 secs

Gaseous Environment	Fe_2O_3/C Ratio	Sample size	Time (s)	Log (dF/dt)			Q(KJ/mol)
				1150 K	1250 K	1300 K	
H_2:CO_2 (1.5:1)	3:1	Big	600	-3.83	-3.45	-2.97	154.07
			2100	-5	-3.74	-2.32	483.68
		Small	600	-5.2	-4.07	-3.008	400.25
			2100	--	-3.83	--	--
	4.5:1	Big	600	-4.44	-3.81	-3.94	108.71
			2100	-4.33	-4.14	-3.69	110.32
		Small	600	-4.5	--	--	--
			2100	-4.495	-4	-3.68	152.32

Gaseous Environment	Fe_2O_3/C ratio	Sample size	Time (s)	Log (dF/dt)			Q(KJ/mol)
				1150 K	1250 K	1300 K	
H_2:CO_2 (3:1)	3:1	Big	600	-5.125	-3.48	-3.3	366.19
			2100	-3.197	-5.30	-3.04	-735.06
		Small	600	-3.5	-3.01	-3.73	-135.18
			2100	-3.17	--	--	--
	4.5:1	Big	600	-4.02	-3.387	-2.92	203.917
			2100	-3.96	-3.45	-5.52	-223.37
		Small	600	-3.3	-3.49	-3.48	-372.42
			2100	-3.62	-3.40	-4.49	-127.59

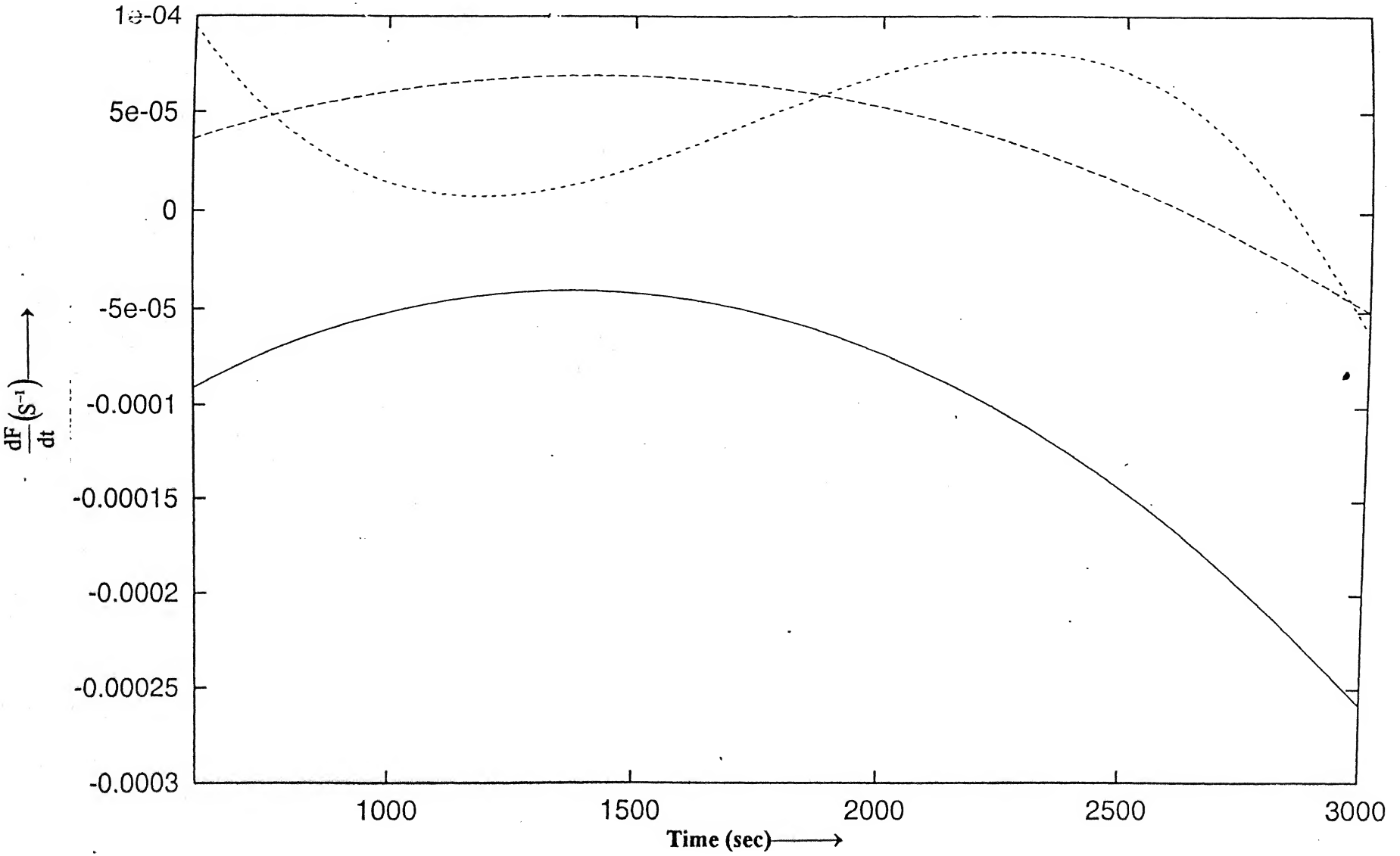

Fig 4.14 : Variation of $\frac{dF}{dt}$ with time for Fe_2O_3/C = 4.5, big sample size at 1150K

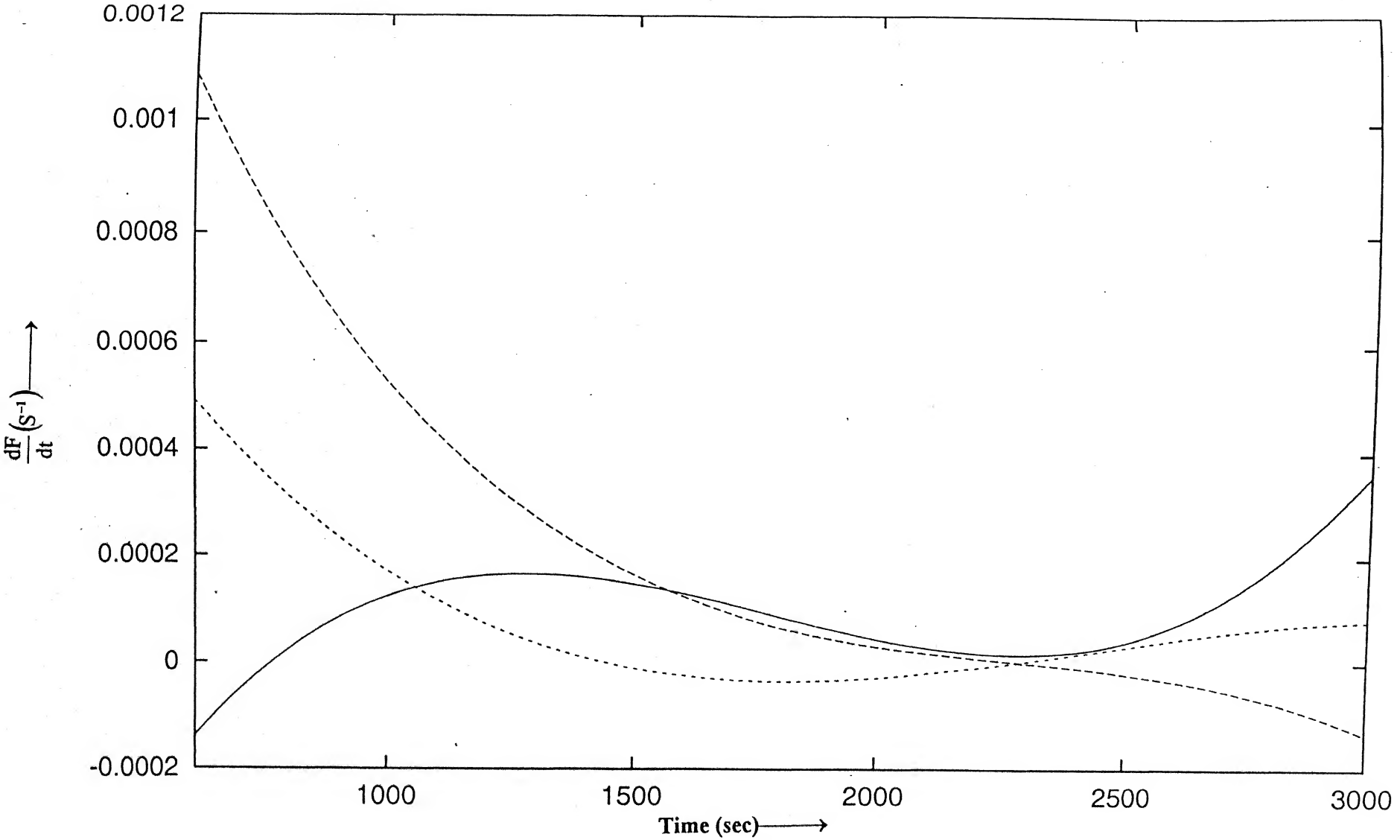

Fig 4.15 : Variation of $\frac{dF}{dt}$ with time for $Fe_2O_3/C = 3$, big sample size at 1300K

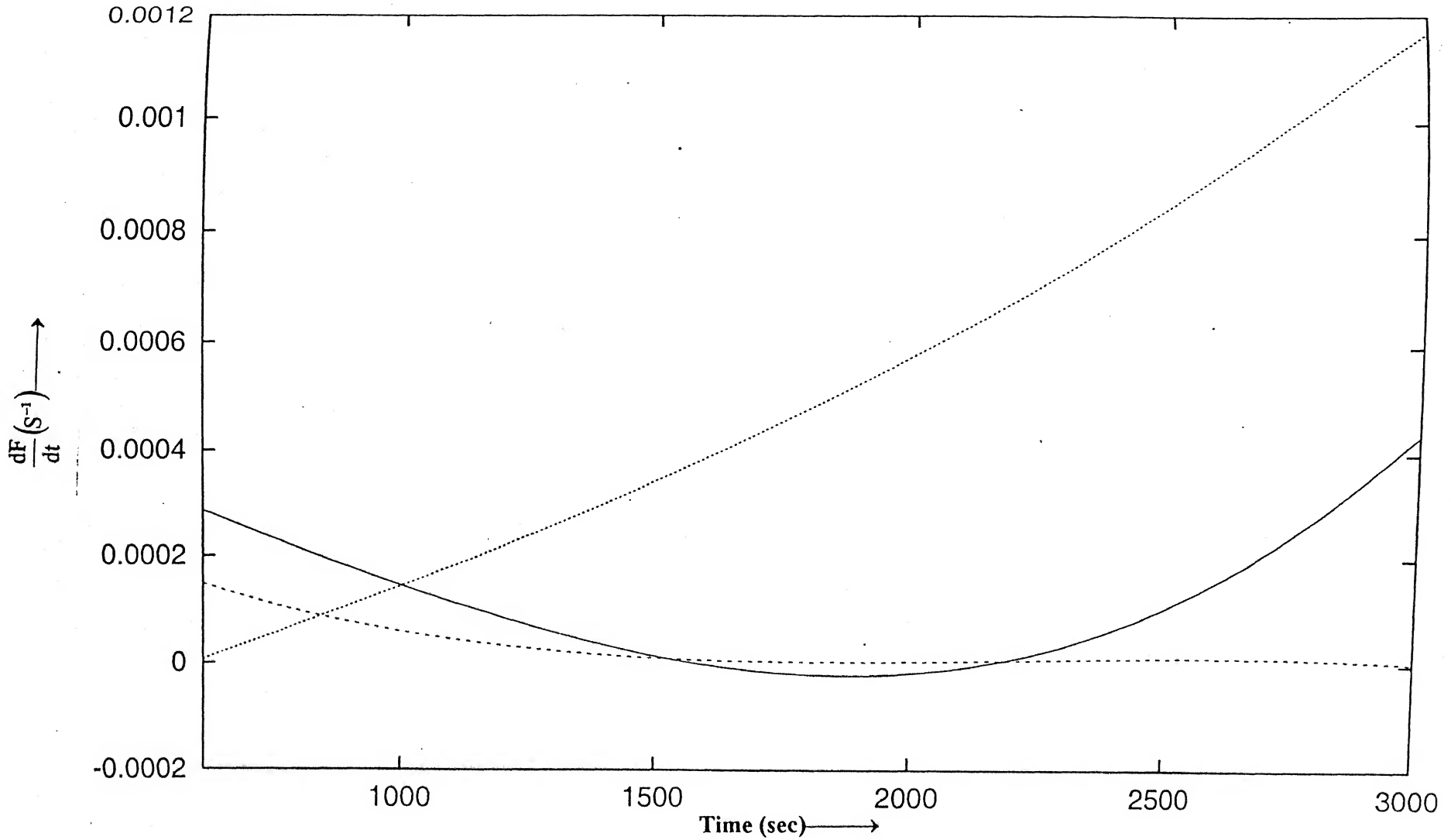

Fig 4.16 : Variation of $\frac{dF}{dt}$ with time for $Fe_2O_3/C = 3$, big sample size at 1150K

Chapter 5

SUMMARY AND CONCLUSIONS

(1) Experiments were conducted with mixtures of fines of blue dust and activated char at 1150, 1250, and 1300 K, and for times of 600, 1200, 1800, 2400, and 3000 seconds.

(2) The dried powder mixtures were taken in two sizes of cylindrical stainless steel crucibles (i.d 1.1 cm and heights of 6 mm and 1 cm). A horizontal tube furnace was employed.

(3) The other variables were

(a) Inlet gas composition – argon, gas mixtures of hydrogen and carbon dioxide with H_2/CO_2 equal to 3 and 1.5.

(b) Fe_2O_3/C mass ratios in the sample of 3 and 4.5.

(4) The total inlet gas flow rate in all atmospheres were kept at 4 cm^3s^{-1} (STP).

(5) The samples were weighed before introduction into the furnace and after taking out from the furnace.

(6) The degree of reduction (F) was determined by subjecting the partially reduced samples through flowing hydrogen at 1023 K for 1 hour. The weight loss in hydrogen was attributed to oxygen removal from unreduced iron oxide.

(7) F versus t data were fitted with polynomial by statistical regression.

(8) F versus t data for inlet gas of H_2/CO_2 equal to 3 exhibited highest degree of reduction in most cases. The gas mixture with H_2/CO_2 equal to 1.5, on the other hand, showed the lowest degree of reduction in most cases. However there were deviations also. Brief explanations have been provided for the behaviour patterns.

(9) At 1300 K, almost complete reduction was observed even under gas mixture with H_2/CO_2 equal to 1.5, although this gas is oxidising to wustite from a thermodynamic point of view.

(10) In view of complex mechanism and kinetics of reactions in the system, dF/dt values cannot be properly explained, although dF/dt is a measure of rate.

(11) Temperature Coefficients (Q) were estimated from dF/dt data. They exhibited wide range, and even negative values.

REFERENCES

(1) Ajay Singh, M.Tech Thesis (to be submitted), I.I.T Kanpur, Dec (1999).

(2) A. Ghosh and S.K Dutta, IIM Metal News, Vol 2, No 2, April (1999).

(3) Frank N. Griscon etal, Alternative Routes to Iron and Steel, 11-13 January, Jamshedpur, (1996), p 75-76.

(4) R.H.Tupkary, Introduction to modern Iron Making p 279-280.

(5) G.Pliego and J.O.Becerra, International Conference on Alternative Routes of Iron and Steel Making (ICARISM'99), 15-17 September, Perth, Australia, p 115-120.

(6) L.Von Bogdandy, H.J.Engell, The reduction of iron ores, p 263, 266-267.

(7) R. Hussain, S. Sneyed and P. Weber, International Conference on Alternative Routes of Iron and Steel Making (ICARISM'99), 15-17 September, Perth, Australia, p 123-126.

(8) A.Ghosh, Alternative routes to Iron and Steel(A) 11-13 January (1996), Jamshedpur, p 25.

(9) F.Oeters and E.Gort, Steel Research, 61(1990), p 385.

(10) Pradip Sandhir and Dr. P.K.Roy, Alternative routes to Iron and Steel(A) 11-13 January (1996), Jamshedpur, p 99-106.

(11) Bhattacharya etal, International Conference on Alternative Routes of Iron and Steel Making (ICARISM'99), 15-17 September, Perth, Australia, p 151.

(12) S.C.Koria, International Conference on Alternative Routes of Iron and Steel Making (ICARISM'99), 15-17 September, Perth, Australia, p 265

(13) A.Ghosh, Alternative routes to Iron and Steel(A) 11-13 January (1996), Jamshedpur, p-17.

(14) A.Ghosh, Alternative routes to Iron and Steel(A) 11-13 January (1996), Jamshedpur, p-27.

(15) A.Ghosh, International Conference on Alternative Routes of Iron and Steel Making (ICARISM'99), 15-17 September, Perth, Australia, p-71.

(16) Lakshman etal, Alternative routes to Iron and Steel(A) 11-13 January (1996), Jamshedpur, p-1.

(17) Amit Chatterjee, Alternative routes to Iron and Steel(A) 11-13 January (1996), Jamshedpur, p-47.

(18) S. K. Dutta, Ph.D Thesis. I.I.T Kanpur, July (1991), p-45.

(19) Bry K and Lu, Iron Making and Steel Making, (1986), p-70.

(20) S. Dutta and A. Ghosh, ISIJ International, Vol. 33, (1993), p-1104.

(21) O.Kubaschewski, E.Li.Evans and C.B.Alcock: Metallurgical Thermochemistry, Vol. 1, fourth edition, Pergamon press, London, (1967).

(22) L.S.Darken and R.W.Gurry, J.Am.Chem. Soc., Vol. 67, (1945), p-1398.

(23) R.C Gupta, A compilation of invited lectures, NMD/ATM, I.I.T Kanpur, 13-16 Nov, (1999), p-40

(24) A.Eberle etal, International Conference on Alternative Routes of Iron and Steel Making (ICARISM'99), 15-17 September, Perth, Australia, p-202.

(25) A.D.Brent etal, International Conference on Alternative Routes of Iron and Steel Making (ICARISM'99), 15-17 September, Perth, Australia, p-112.

(26) R.Husain etal, International Conference on Alternative Routes of Iron and Steel Making (ICARISM'99), 15-17 September, Perth, Australia, p-112.

(27) S.K.Gupta and A.K.Lahiri, Alternative routes to Iron and Steel(A) 11-13, January (1996), Jamshedpur, p-7.

(28) SIMA, October-December, (1998), p-12-13.

(29) K.K.Prasad etal, Alternative routes to Iron and Steel(B), 11-13, January (1996), Jamshedpur, p-28.

Table A 1.1 : Experimental data in argon

Experiment Code	Time(s)	Ws(gm)	Wio(gm)	F	Value of Co-efficients a	b ($x10^5$)	c ($x10^7$)	d ($x10^{11}$)	e ($x10^{14}$)
a3011arb	600	0.9078	0.1929	0.335	0.10	49.20	-1.47	-4.12	1.79
	1200	0.9014	0.1916	0.444					
	1800	0.9566	0.2033	0.456					
	2400	0.9149	0.1945	0.459					
	3000	0.9009	0.1915	0.593					
a3012arb	600	0.6854	0.1457	0.619	0.66	-15.75	1.75	-6.18	0.76
	1200	0.7855	0.1669	0.635					
	1800	0.7947	0.1689	0.667					
	2400	0.9006	0.1914	0.692					
	3000	0.8513	0.1809	0.713					
a3013arb	600	0.8824	0.1875	0.653	1.01	-121.31	13.20	-53.55	7.50
	1200	0.8558	0.1819	0.687					
	1800	0.9398	0.1998	0.769					
	2400	0.8746	0.1859	0.790					
	3000	0.9266	0.1969	0.873					
a4511arb	600	1.0405	0.2419	0.402	0.47	-19.96	1.56	-2.79	0.0
	1200	0.9316	0.2165	0.420					
	1800	1.0147	0.2359	0.444					
	2400	0.9174	0.2132	0.517					
	3000	0.8391	0.1950	0.524					
a4512arb	600	0.9789	0.2275	0.630	0.69	-17.75	1.51	-2.75	0.0
	1200	0.9664	0.2246	0.651					
	1800	0.9724	0.2260	0.690					
	2400	1.115	0.2592	0.757					
	3000	0.8497	0.1975	0.770					
a4513arb	600	1.1542	0.2683	0.673	0.48	49.60	-3.46	10.65	-1.13
	1200	1.0165	0.2363	0.735					
	1800	1.129	0.2624	0.751					
	2400	0.9527	0.2215	0.771					
	3000	1.1105	0.2581	0.809					

Table A 1.1 (contd..)

Experiment Code	Time(s)	Ws(gm)	Wio(gm)	F	Value of Co-efficients a	b ($x10^5$)	c ($x10^7$)	d ($x10^{11}$)	e ($x10^{14}$)
	600	0.4868	0.1034	0.438					
	1200	0.4833	0.1027	0.454					
a3011ars	1800	0.2486	0.0528	0.485	0.63	-65.28	7.37	-31.95	4.84
	2400	0.517	0.1099	0.494					
	3000	0.4387	0.0932	0.594					
	600	0.486	0.1033	0.437					
	1200	0.2466	0.0524	0.569					
a3012ars	1800	0.396	0.0841	0.625	0.25	31.49	0.40	-9.15	2.02
	2400	0.4658	0.0990	0.641					
	3000	0.3773	0.0802	0.721					
	600	0.5046	0.1072	0.688					
	1200	0.3768	0.0801	0.710					
a3013ars	1800	0.4648	0.0988	0.744	0.69	-2.67	0.62	-2.70	0.60
	2400	0.3954	0.0840	0.803					
	3000	0.4834	0.1027	0.917					
	600	0.4573	0.1063	0.446					
	1200	0.4592	0.1067	0.486					
a4511ars	1800	0.4864	0.1130	0.500	0.35	21.41	-1.17	2.86	-0.25
	2400	0.5626	0.1308	0.504					
	3000	0.5804	0.1349	0.510					
	600	0.5815	0.1351	0.506					
	1200	0.4964	0.1154	0.579					
a4512ars	1800	0.4696	0.1091	0.625	0.46	-0.71	1.88	-10.4	1.64
	2400	0.5213	0.1212	0.637					
	3000	0.4004	0.0930	0.659					
	600	0.532	0.1236	0.540					
	1200	0.5573	0.1295	0.613					
a4513ars	1800	0.5038	0.1171	0.729	0.94	-142.78	16.20	-65.85	8.99
	2400	0.5161	0.1199	0.732					
	3000	0.4495	0.1045	0.749					

Table A 1.2 : Experimental data in H_2:CO_2 = 1.5:1

Experiment Code	Time(s)	Ws(gm)	Wio(gm)	F	Value of Co-efficients a	b ($x10^5$)	c ($x10^7$)	d ($x10^{11}$)	e ($x10^{14}$)
	600	0.7698	0.1636	0.343					
	1200	0.8103	0.1722	0.392					
a3011H2b	1800	0.8181	0.1739	0.400	0.19	40.02	-2.81	8.68	-0.97
	2400	0.7823	0.1663	0.405					
	3000	0.7685	0.1633	0.411					
	600	0.7233	0.1537	0.307					
	1200	0.7256	0.1542	0.435					
a3012H2b	1800	0.7683	0.1633	0.503	-0.06	96.52	-7.17	25.28	-3.06
	2400	0.7876	0.1674	0.601					
	3000	0.699	0.1486	0.723					
	600	0.6787	0.1442	0.458					
	1200	0.8524	0.1812	0.860					
a3013H2b	1800	0.7594	0.1614	0.970	-0.58	253.32	-15.72	44.62	-4.89
	2400	0.7945	0.1689	0.986					
	3000	0.6815	0.1448	0.954					
	600	0.8289	0.1927	0.327					
	1200	0.8404	0.1953	0.350					
a4511H2b	1800	0.9944	0.2311	0.409	0.321	-2.80	0.68	-1.59	0.00
	2400	0.9112	0.2118	0.418					
	3000	0.7703	0.1790	0.420					
	600	0.7755	0.1803	0.407					
	1200	0.8995	0.2091	0.459					
a4512H2b	1800	0.9482	0.2204	0.476	0.26	35.70	-2.10	4.11	0.17
	2400	0.9668	0.2247	0.526					
	3000	0.845	0.1964	0.680					
	600	0.7747	0.1801	0.485					
	1200	0.8217	0.1910	0.623					
a4513H2b	1800	0.8313	0.1932	0.699	0.47	-8.49	2.05	-4.30	0.00
	2400	0.859	0.1997	0.886					
	3000	0.8693	0.2021	0.899					

Table A 1.2 (contd..)

Experiment Code	Time(s)	Ws(gm)	Wio(gm)	F	Value of Co-efficients a	b ($x10^5$)	c ($x10^7$)	d ($x10^{11}$)	e ($x10^{14}$)
a3011H2s	600	0.4498	0.0956	0.361	0.39	-16.06	2.53	-11.35	1.64
	1200	0.4074	0.0866	0.398					
	1800	0.3676	0.0781	0.429					
	2400	0.3183	0.0676	0.434					
	3000	0.3802	0.0808	0.445					
a3012H2s	600	0.3393	0.0721	0.434	0.33	26.28	-1.98	5.91	-0.16
	1200	0.35	0.0744	0.464					
	1800	0.4207	0.0894	0.498					
	2400	0.3594	0.0764	0.588					
	3000	0.4835	0.1027	0.806					
a3013H2s	600	0.337	0.0716	0.507	-0.34	191.44	-8.90	13.23	-0.0049
	1200	0.3592	0.0763	0.929					
	1800	0.3548	0.0754	0.946					
	2400	0.3833	0.0814	0.978					
	3000	0.305	0.0648	0.947					
a4511H2s	600	0.3602	0.0837	0.455	0.43	6.22	-0.33	0.81	0.00
	1200	0.4631	0.1076	0.469					
	1800	0.4285	0.0996	0.482					
	2400	0.4383	0.1019	0.501					
	3000	0.4135	0.0961	0.540					
a4512H2s	600	0.4016	0.0933	0.432	0.60	-0.65.10	7.99	-38.17	6.49
	1200	0.4619	0.1073	0.454					
	1800	0.4472	0.1039	0.483					
	2400	0.478	0.1111	0.528					
	3000	0.4028	0.0936	0.802					
a4513H2s	600	0.3596	0.0836	0.542	0.77	-69.30	5.81	-11.12	0.00
	1200	0.4913	0.1142	0.581					
	1800	0.4734	0.1100	0.764					
	2400	0.4193	0.0974	0.915					
	3000	0.4056	0.0943	0.922					

Table A 1.3 : Experimental data in $H_2:CO_2 = 3:1$

Experiment Code	Time(s)	Ws(gm)	Wio(gm)	F	Value of Co-efficients a	b ($x10^5$)	c ($x10^7$)	d ($x10^{11}$)	e ($x10^{14}$)
	600	0.7642	0.1624	0.456					
	1200	0.7926	0.1685	0.463					
a3011H1b	1800	0.8867	0.1885	0.509	0.51	-15.74	1.21	-1.99	0.057
	2400	0.7808	0.1659	0.573					
	3000	0.886	0.1883	0.635					
	600	0.9763	0.2075	0.414					
	1200	0.9832	0.2090	0.653					
a3012H1b	1800	0.8981	0.1909	0.808	0.39	-39.53	10.04	-50.03	7.58
	2400	0.9568	0.2034	0.823					
	3000	0.9237	0.1963	0.872					
	600	1.0049	0.2136	0.790					
	1200	0.9281	0.1973	0.944					
a3013H1b	1800	0.923	0.1962	0.947	0.26	137.46	-9.65	28.25	-2.89
	2400	0.9379	0.1993	0.942					
	3000	0.8949	0.1902	0.980					
	600	1.0969	0.2550	0.490					
	1200	1.0616	0.2468	0.509					
a4511H1b	1800	1.0734	0.2495	0.523	0.34	45.84	-4.62	19.75	-2.86
	2400	1.0892	0.2532	0.565					
	3000	1.1471	0.2667	0.580					
	600	1.0575	0.2458	0.427					
	1200	1.0227	0.2377	0.498					
a4512H1b	1800	0.9943	0.2311	0.539	-0.26	214.47	-21.69	90.95	-12.74
	2400	1.0089	0.2345	0.737					
	3000	0.9954	0.2314	0.884					
	600	0.833	0.1936	0.556					
	1200	0.9292	0.2160	0.930					
a4513H1b	1800	0.9673	0.2248	0.939	-0.71	325.40	-22.57	65.46	-6.74
	2400	0.8215	0.1909	0.907					
	3000	0.9507	0.2210	0.948					

Table A 1.3 (contd..)

Experiment Code	Time(s)	Ws(gm)	Wio(gm)	F	Value of Co-efficients a	b ($x10^5$)	c ($x10^7$)	d ($x10^{11}$)	e ($x10^{14}$)
	600	0.3974	0.0844	0.446					
	1200	0.4843	0.1029	0.472					
a3011H1s	1800	0.3956	0.0841	0.536	-0.26	236.68	-26.49	120.32	-18.09
	2400	0.4192	0.0891	0.792					
	3000	0.4146	0.0881	0.830					
	600	0.5187	0.1102	0.412					
	1200	0.5203	0.1106	0.799					
a3012H1s	1800	0.4883	0.1038	0.889	-0.41	180.07	-7.57	6.67	1.17
	2400	0.5011	0.1065	0.860					
	3000	0.519	0.1103	0.926					
	600	0.4583	0.0974	0.901					
	1200	0.4863	0.1033	0.970					
a3013H1s	1800	0.4785	0.1017	0.981	0.72	41.19	-2.23	4.40	-0.18
	2400	0.4632	0.0984	0.976					
	3000	0.4304	0.0915	0.993					
	600	0.5477	0.1273	0.413					
	1200	0.471	0.1095	0.513					
a4511H1s	1800	0.5775	0.1342	0.531	-0.26	200.43	-18.59	72.08	-9.45
	2400	0.5592	0.1300	0.665					
	3000	0.5787	0.1345	0.820					
	600	0.5575	0.1296	0.392					
	1200	0.5224	0.1214	0.495					
a4512H1s	1800	0.474	0.1102	0.620	-0.07	141.41	-14.25	65.35	-9.97
	2400	0.4796	0.1115	0.839					
	3000	0.5215	0.1212	0.912					
	600	0.5439	0.1264	0.730					
	1200	0.4444	0.1033	0.859					
a4513H1s	1800	0.4541	0.1055	0.988	0.47	50.47	-1.58	1.43	0.00
	2400	0.4557	0.1059	0.958					
	3000	0.4243	0.0986	0.964					